5. UNDERGROUND CABLES

There is such a large variety of cable designs on the market, that it is difficult, if not impossible, to develop one computer program which can calculate the parameters R', L', C' for any type of cable.

For lower voltage ratings, the cables are usually unscreened and insulated with polyvinyl chloride. An example of a three-phase 1 kV cable with neutral conductor and armor is shown in Fig. 5.1.

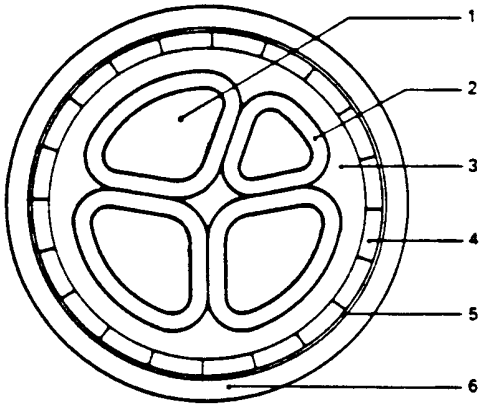

Fig. 5.1 - Armored 1 kV cable (1 = stranded conductor, 2 = insulation, 3 = bedding, 4 = flat steel wire armor, 5 = helical steel tape, 6 = plastic outer sheath). Reprinted by permission from Siemens Catalog 1980

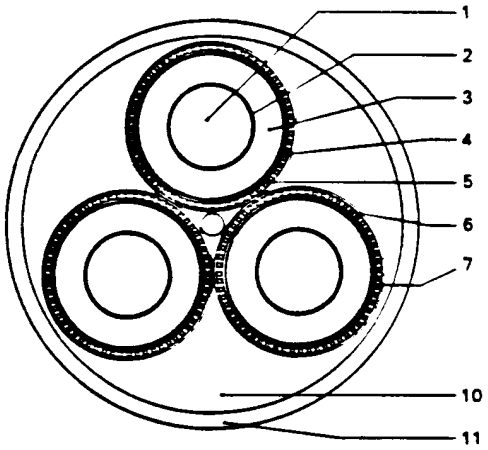

Fig. 5.2 - 12 to 35 kV distribution cable with concentric neutral conductors (1 = stranded conductor, 2, 4 = conductive layers, 3 = plastic insulation , 5 = conductive tape, 6 = concentric neutral conductors, 7 = helical copper tape, 10 = inner sheath, 11 = plastic outer sheath). Reprinted by permission from Siemens Catalog 1980

At the distribution voltage level, the cables are usually screened with concentric neutral conductors, as shown in Fig. 5.2.

At the transmission voltage level, two types of cables are in widespread use today, namely the pipe-type cable (Fig. 5.3) and the self-contained cable (Fig. 5.4). In the pipe-type cable, three paper-insulated oil-impregnated cables are drawn into a steel pipe at the construction site. The helical skid wires make it easier to pull the cables. After evacuation, the pipe is filled with oil and pressurized to a high pressure of approx. 1.5 kPa. Pipe-type cables are used for voltages from 69 to 345 kV, with 550 kV cables under development. The typical

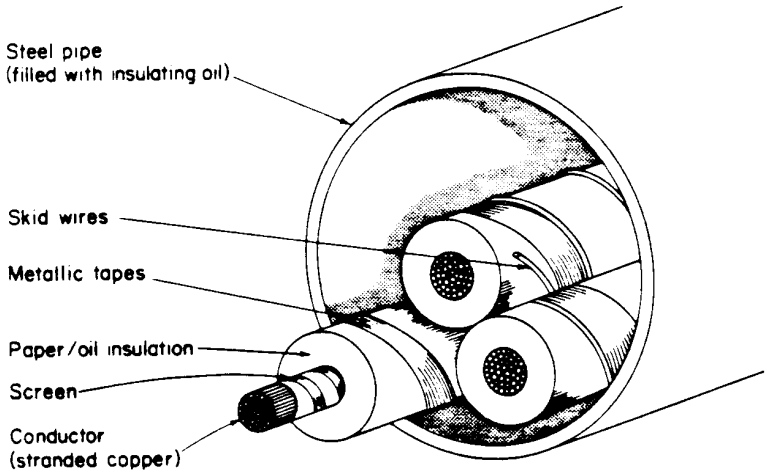

Fig. 5.3 - Pipe-type oil-filled cable [148]. © 1979 John Wiley & Sons, Ltd. Reprinted by permission of John Wiley & Sons, Ltd

self-contained oil-filled cable is a single-core cable (Fig. 5.4). Its stranded core conductor has a hollow duct which is filled with oil and kept pressurized with low-pressure bellow-type expansion tanks. Underground and submarine self-contained cables are essentially identical, except that underground cables do not always have an armor.

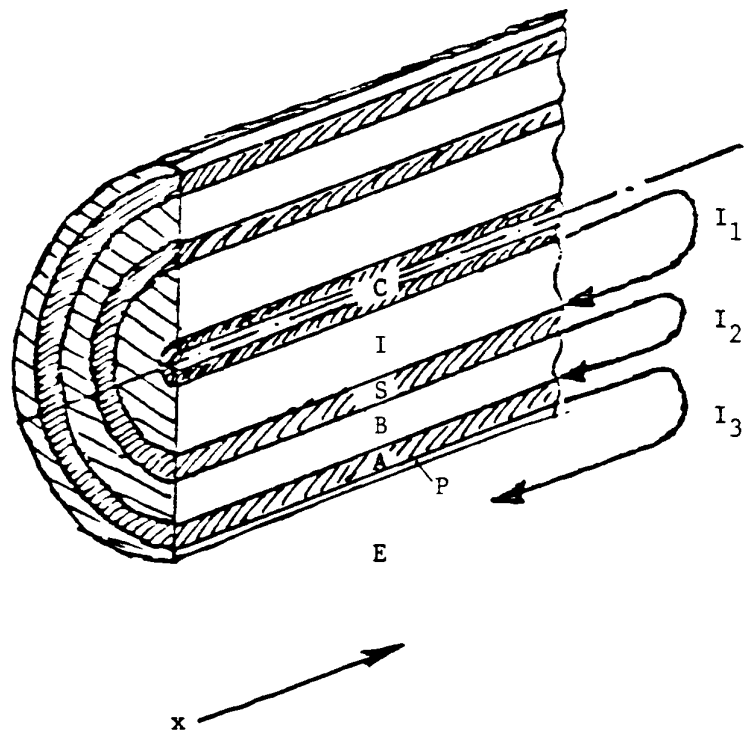

Fig. 5.4 - Single-core self-contained cable (C = stranded core conductor with oil-filled duct, I = paper insulation, S = metallic sheath, B = bedding, A = armor, P = plastic sheath). Details of conductive layers left out

Gas-insulated systems with compressed SF_6 gas are used for compact substation designs. The busses in such substations consist of tubular conductors inside a metallic sheath, with the conductors held in place by plastic spacers at certain intervals (Fig. 5.5). SF_6-busses are in use in lengths of up to 300 m. A similar design can be used for cables, but SF_6-cables are still experimental, with the sheath usually being corrugated. In EMTP studies, such relatively short

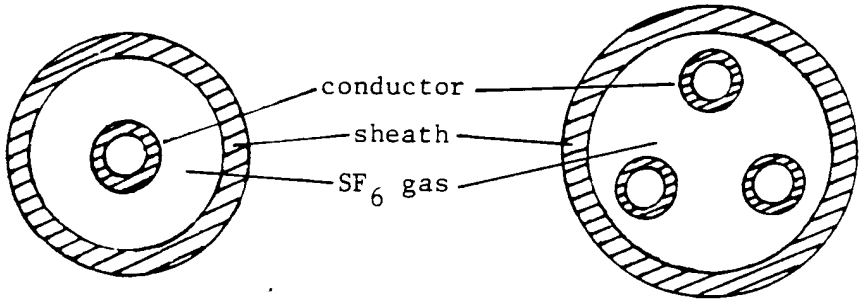

(a) Single-phase (b) Three-phase

Fig. 5.5 - SF_6 bus

busses can often be ignored, or represented as a lumped capacitance. Only in studies of fast transients with high frequencies must SF_6-busses be represented as transmission lines. Since the single-phase geometry is essentially

similar to that of a self-contained cable, and since the three-phase geometry is similar to that of a pipe-type cable, no special programs are needed to handle SF_6-busses or cables, except that the three-phase arrangement of Fig. 5.5(b) has no electrostatic screens as in the case of a pipe-type cable of Fig. 5.3.

Fig. 5.1 to 5.5 are only a few examples for the large variety of cable designs. The support routine CABLE CONSTANTS was developed by A. Ametani essentially for the coaxial single-core cable design of Fig. 5.4 and 5.5(a), and later expanded for the pipe-type cable of Fig. 5.3 and for the three-phase SF_6-busses of Fig. 5.5(b). At this time, there is no support routine for the types of lower voltage cables shown in Fig. 5.1 and 5.2, but calculation methods applicable to such non-coaxial arrangements are briefly discussed in Section 5.7.

5.1 Single-Core Cables

The cable parameters of coaxial arrangements, as in Fig. 5.4, are derived in the form of equations for coaxial loops [150, 152]. In Fig. 5.4, loop 1 is formed by the core conductor C and the metallic sheath S as return, loop 2 by the metallic sheath S and metallic armor A as return, and finally loop 3 by the armor A and either earth or sea water as return.

5.1.1 Series Impedances

The series impedances of the three loops are described by three coupled equations

$$-\begin{bmatrix} \frac{dV_1}{dx} \\ \frac{dV_2}{dx} \\ \frac{dV_3}{dx} \end{bmatrix} = \begin{bmatrix} Z'_{11} & Z'_{12} & 0 \\ Z'_{21} & Z'_{22} & Z'_{23} \\ 0 & Z'_{32} & Z'_{33} \end{bmatrix} \begin{bmatrix} I_1 \\ I_2 \\ I_3 \end{bmatrix} \tag{5.1}$$

The self impedance Z'_{11} of loop 1 consists of 3 parts,

$$Z'_{11} = Z'_{\text{core-out}} + Z'_{\text{core/sheath-insulation}} + Z'_{\text{sheath-in}} \tag{5.2}$$

with

$Z'_{\text{core-out}}$ = internal impedance (per unit length) of tubular core conductor with return path outside the tube (through sheath here)

$Z'_{\text{core/sheath-insulation}}$ = impedance (per unit length) of insulation between core and sheath, and

$Z'_{\text{sheath-in}}$ = internal impedance (per unit length) or tubular sheath with return path inside the tube (through core conductor here).

Similarly,

$$Z'_{22} = Z'_{\text{sheath-out}} + Z'_{\text{sheath/armor insulation}} + Z'_{\text{armor-in}} \tag{5.3}$$

and

$$Z'_{33} = Z'_{armor\text{-}out} + Z'_{armor/earth\text{-}insulation} + Z'_{earth} \tag{5.4}$$

with analogous definitions as for Eq. (5.2). The coupling impedances $Z'_{12} = Z'_{21}$ and $Z'_{23} = Z'_{32}$ are negative because of opposing current directions (I_2 in negative direction in loop 1, I_3 in negative direction in loop 2),

$$Z'_{12} = Z'_{21} = -Z'_{sheath\text{-}mutual} \tag{5.5a}$$

$$Z'_{23} = Z'_{32} = -Z'_{armor\text{-}mutual} \tag{5.5b}$$

with $Z'_{sheath\text{-}mutual}$ = mutual impedance (per unit length) of tubular sheath between the inside loop 1 and the outside loop 2, and

$Z'_{armor\text{-}mutual}$ = mutual impedance (per unit length) of tubular armor between the inside loop 2 and the outside loop 3.

Finally, $Z'_{13} = Z'_{31} = 0$ because loop 1 and loop 3 have no common branch.

The simplest terms to calculate are the impedances of the insulation, which are simply

$$Z'_{insulation} = j\omega \frac{\mu_0}{2\pi} \ln\frac{r}{q} \tag{5.6}$$

with μ_0 = permeability of insulation ($\mu_0 = 2 \bullet 10^{-4}$ H/km),

r = outside radius of insulation,
q = inside radius of insulation,] in identical units (e.g. in mm)

If the insulation is missing, e.g., between armor and earth, then $Z'_{insulation} = 0$.

The internal impedance and the mutual impedance of a tubular conductor with inside radius q and outside radius r (Fig. 4.5) are a function of frequency, and are found with modified Bessel functions [149].

$$Z'_{tube\text{-}in} = \rho m/2\pi qD \{I_0(mq)\, K_1(mr) + K_0(mq)\, I_1(mr)\} \tag{5.7a}$$

$$Z'_{tube\text{-}out} = \rho m/2\pi rD \{I_0(mr)\, K_1(mq) + K_0(mr)\, I_1(mq)\} \tag{5.7b}$$

$$Z'_{tube\text{-}mutual} = \rho/2\pi qrD \tag{5.7c}$$

$$\text{with } D = I_1(mr)\, K_1(mq) - I_1(mq)\, K_1(mr) \tag{5.7d}$$

The parameter

$$m = \sqrt{j\omega\mu/\rho} \tag{5.7e}$$

is the reciprocal of the complex depth of penetration (OVERLINE) p defined earlier in Eq. (4.5).

A subroutine SKIN for calculating the impedance $Z'_{tube\text{-}out}$ of Eq. (5.7b) was developed at BPA for the support routine LINE CONSTANTS, and later modified at UBC to "TUBE" for the calculation of $Z'_{tube\text{-}in}$ and $Z'_{tube\text{-}mutual}$ as well. All arguments of the modified Bessel functions I_0, I_1, K_0, K_1 are complex numbers with a phase angle of 45° because of Eq. (5.7e). In such a case, the following real functions of a real variable can be used instead:

$$ber(x) + jbei(x) = I_0(x\sqrt{j})$$

$$ber'(x) + jbei'(x) = \sqrt{j}I_1(x\sqrt{j}) \tag{5.8}$$

$$ker(x) + jkei(x) = K_0(x\sqrt{j})$$

$$ker'(x) + jkei'(x) = -\sqrt{j}K_1(x\sqrt{j})$$

These functions are evaluated numerically with the polynomial approximations of Eq. (9.11.1) to (9.11.14) of [149]. For arguments $x \leq 8$, the absolute error is $< 10^{-7}$, whereas for arguments $x > 8$, the relative error is $< 3 \bullet 10^{-7}$. To avoid too large numbers in the numerator and denominator for large arguments of x, the expressions f(x) and g(x) in Eq. (9.22.9) and (9.11.10) of [149] are multiplied with exp $(- 1 + j/\sqrt{2}\, x)$. If both arguments mq and mr have absolute values greater than 8, then in addition to the above multiplication, the K_0- and K_1- functions are further multiplied by exp (2mq) to avoid indefinite terms 0/0 for very large arguments.

When the support routine CABLE CONSTANTS was developed, subroutine TUBE did not yet exist, and A. Ametani chose slightly different polynomial approximations for the functions I_0, I_1, K_0, K_1 in Eq. (5.7). He uses Eq. (9.8.1) to (9.8.8) of [149] instead, with the accuracy being more or less the same as in the polynomials used in subroutine TUBE.

Simpler formulas with hyperbolic cotangent functions in place of Eq. (5.7) were developed by M. Wedepohl [150], which also give fairly accurate answers as long as the condition $(r-q)/(r+q) < 1/8$ is fulfilled. This was verified by the author for the data of a 500 kV submarine cable.

The only term which still remains to be defined is Z'_{earth} in Eq. (5.4). This is the earth or sea return impedance of a single buried cable, which is discussed in more detail in Section 5.3.

Submarine cables always have an armor, while underground cables may only have a sheath. The armor often consists of spiralled steel wires, which can be treated as a tube of equal cross section with $\mu_r = 1$, without too much error (153]. A more accurate representation is discussed in [151].

Eq. (5.1) is not yet in a form suitable for EMTP models, in which the voltages and currents of the core, sheath, and armor must appear, in place of loop voltages and currents. The transformation is achieved by introducing the terminal conditions

$$\begin{aligned} V_1 &= V_{core} - V_{sheath} & & I_1 = I_{core} \\ V_2 &= V_{sheath} - V_{armor} & \text{and} \quad & I_2 = I_{sheath} + I_{core} \\ V_3 &= V_{armor} & & I_3 = I_{armor} + I_{sheath} + I_{core} \end{aligned} \tag{5.9}$$

where V_{core} = voltage from core to ground,

V_{sheath} = voltage from sheath to ground,

V_{armor} = voltage from armor to ground.

By adding row 2 and 3 or Eq. (5.1) to the first row, and by adding row 3 to the second row, we obtain

$$-\begin{bmatrix} dV_{core}/dx \\ dV_{sheath}/dx \\ dV_{armor}/dx \end{bmatrix} = \begin{bmatrix} Z'_{cc} & Z'_{cs} & Z'_{ca} \\ Z'_{sc} & Z'_{ss} & Z'_{sa} \\ Z'_{ac} & Z'_{as} & Z'_{aa} \end{bmatrix} \begin{bmatrix} I_{core} \\ I_{sheath} \\ I_{armor} \end{bmatrix} \tag{5.10}$$

with $Z'_{cc} = Z'_{11} + 2Z'_{12} + Z'_{22} + 2Z'_{23} + Z'_{33}$,

$Z'_{cs} = Z'_{sc} = Z'_{12} + Z'_{22} + 2Z'_{23} + Z'_{33}$,

$Z'_{ca} = Z'_{ac} = Z'_{sa} = Z'_{as} = Z'_{23} + Z'_{33}$,

$Z'_{ss} = Z'_{22} + 2Z'_{23} + Z'_{33}$,

$Z'_{aa} = Z'$ (5.10b)

Some authors use equivalent circuits without mutual couplings, in place of the matrix representation of Eq. (5.10) with self impedances (diagonal elements) and mutual impedances (off-diagonal elements). For example, [150] shows the equivalent circuit of Fig. 5.6 for a single-core cable without armor, which is essentially the same as the TNA four-conductor representation of overhead lines in Fig. 4.28.

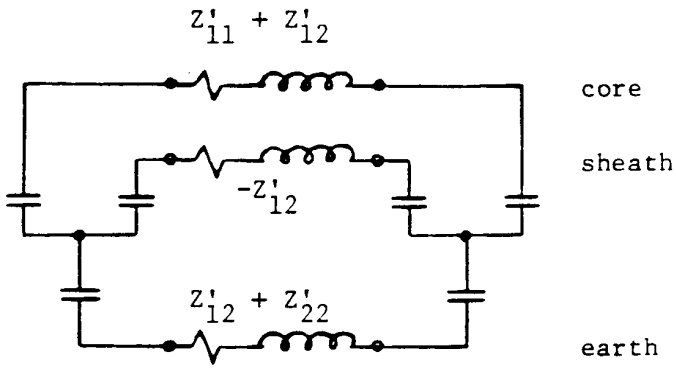

Fig. 5.6 - Three conductor π-circuit suitable for TNA's

5.1.2 Shunt Admittances

For the current changes along the cable of Fig. 5.4, the loop equations are not coupled,

$$\begin{aligned} -dI_1/dx &= (G'_1 + j\omega C'_1)V_1 \\ -dI_2/dx &= (G'_2 + j\omega C'_2)\ V_2 \\ -dI_3/dx &= (G'_3 + j\omega C'_3)V_3 \end{aligned} \tag{5.11}$$

G'_i and C'_i are the shunt conductance and shunt capacitance per unit length for each insulation layer. If there is no insulation (e.g., armor in direct contact with the earth), then replace Eq. (5.11) by

$$V_i = 0 \tag{5.12}$$

The shunt capacitance of tubular insulation with inside radius q and outside radius r is

$$C' = \frac{2\pi\varepsilon_0\varepsilon_r}{\ln\frac{r}{q}} \tag{5.13}$$

with ε_0 = absolute permittivity or dielectric constant of free space (ε_0 defined in Eq. (4.22)) and ε_r = relative permittivity or relative dielectric constant of the insulation material. Typical values for ε_r are shown in Table 5.1 [54].

Table 5.1 - Relative permittivity and loss factor of insulation material [54]. Reprinted by permission of Springer-Verlag and the authors

Insulation Material	Relative Permittivity at 20°C	Loss Factor tanδ at 50 Hz and 20°C
butyl rubber	3.0 to 4.0	0.05
insulating oil	2.2 to 2.8	0.001 to 0.002
oil-impregnated paper	3.3 to 4.2	0.003 to 0.008
polyvinyl chloride	3.0 to 4.0	0.02 to 0.10
polyethylene	2.3	0.0002
crosslinked polyethylene	2.4	0.0004

The shunt conductance G' is ignored in the support routine CABLE CONSTANTS, which is probably reasonable in most cases. It cannot be ignored, however, if buried pipelines are to be modelled as cables, as explained in Section 5.6. If values for G' are available for cables, it is normally in the form of a dielectric loss angle δ or loss factor tanδ. Then

$$G' = \omega C' \bullet \tan\delta \tag{5.14}$$

Typical values for tanδ are shown in Table 5.1. In the literature on electromagnetics, the shunt conductance is usually included by assuming that ε_r in Eq. (5.13) is a complex number $\varepsilon_r = \varepsilon' - j\varepsilon''$, with Eq. (5.13) rewritten as

$$G' + j\omega C' = \frac{j\omega 2\pi\varepsilon_0}{\ln\frac{r}{q}}(\varepsilon' - j\varepsilon'') \tag{5.15}$$

For cross-linked polyethylene, both ε' and ε" are more or less constant up to 100 mHz [168], with the typical values of Table 5.1. For oil-impregnated paper insulation, both ε' and ε" vary with frequency. Measured values between 10 kHz and 100 mHz [154] showed variations in ε' of approximately 20%, whereas ε" varied much more. Fig. 5.7 shows the variations which can be expressed as a function of frequency with the empirical formula

$$\varepsilon_r = 2.5 + \frac{0.94}{(1+j\omega 6\cdot 10^{-9})^{0.315}} \tag{5.16}$$

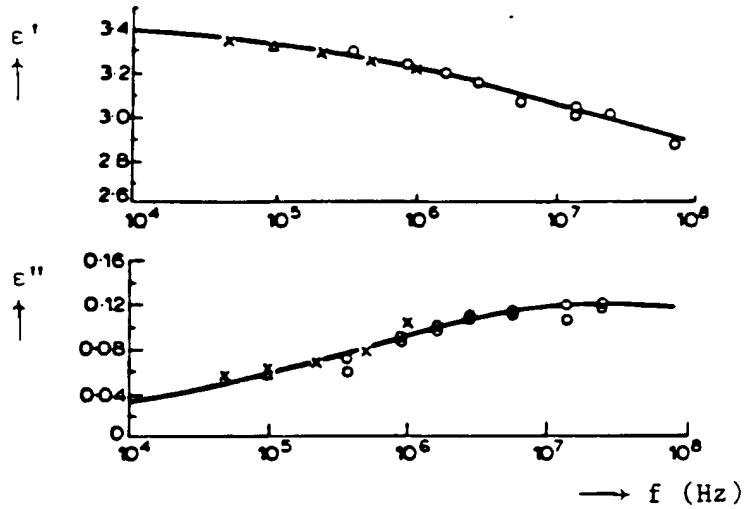

Fig. 5.7 - Measured values of ϵ' and ϵ" for a cable with oil-impregnated paper insulation at 20°C [154]. Reprinted by permission of IEE and the authors

The support routine CABLE CONSTANTS now assumes ε" = 0 and ε' being constant, but it could easily be changed to include empirical formulas based on measurements, such as Eq. (5.16). At this time, formulas based on theory are not available because the frequency-dependent behavior of dielectrics is too complicated. Except for very short pulses (< 5 μs), the dielectric losses are of little importance for the attenuation [154], and using a constant ε' with ε" = 0 should therefore give reasonable answers in most cases.

Again, Eq. (5.11) is not yet in a form suitable for EMTP models. With the conditions of Eq. (5.9), they are transformed to

$$-\begin{bmatrix} dI_{core}/dx \\ dI_{sheath}/dx \\ dI_{armor}/dx \end{bmatrix} = \begin{bmatrix} Y'_1 & -Y'_1 & 0 \\ -Y'_1 & Y'_1+Y'_2 & -Y'_2 \\ 0 & -Y'_2 & Y'_2+Y'_3 \end{bmatrix} \begin{bmatrix} V_{core} \\ V_{sheath} \\ V_{armor} \end{bmatrix} \tag{5.17}$$

where $Y'_i = G'_i + j\omega C'_i$.

5.2 Parallel Single-Core Cables

There are not many cases where single-core cables can be represented with single-phase models. A notable exception is the submarine cable system, where the individual cables are laid so far apart (to reduce the risk of anchors damaging more than one phase) that coupling between the phases can be ignored. In general, the three

single-core cables of a three-phase underground installation are laid close together so that coupling between the phases must be taken into account.

If we start out with loop analysis, then it is apparent that it is only the most outer loops (armor with earth return, or sheath with earth return in the absence of armor) through which the phases become coupled. The magnetic field outside the cable produced by loop 1 and 2 in Fig. 5.4 is obviously zero, because the field created by I_1 in the core is exactly cancelled by the

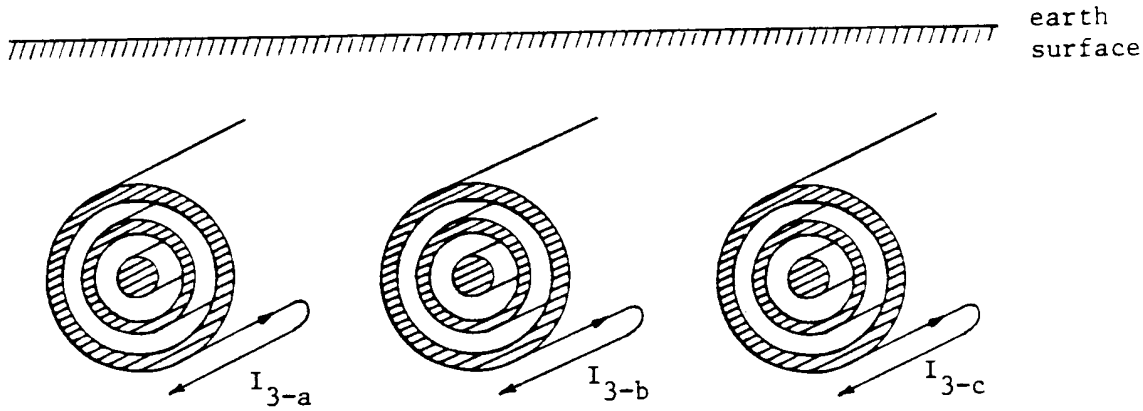

Fig. 5.8 - Three single-core cables

returning current I_1 in the sheath, etc. The first two equations in (5.1) are therefore still valid, whereas the third equation now has coupling terms among the three phases a, b, c, or

$$\left[Z'_{loop}\right] = \begin{bmatrix} \begin{bmatrix} Z'_{11}a & Z'_{12}a & 0 \\ Z'_{21}a & Z'_{22}a & Z'_{23}a \\ 0 & Z'_{32}a & Z'_{33}a \end{bmatrix} & \begin{bmatrix} 0 & 0 & 0 \\ 0 & 0 & 0 \\ 0 & 0 & Z'_{ab} \end{bmatrix} & \begin{bmatrix} 0 & 0 & 0 \\ 0 & 0 & 0 \\ 0 & 0 & Z'_{ac} \end{bmatrix} \\ & \begin{bmatrix} Z'_{11}b & Z'_{12}b & 0 \\ Z'_{21}b & Z'_{22}b & Z'_{23}b \\ 0 & Z'_{32}b & Z'_{33}b \end{bmatrix} & \begin{bmatrix} 0 & 0 & 0 \\ 0 & 0 & 0 \\ 0 & 0 & Z'_{bc} \end{bmatrix} \\ \textit{symmetric} & & \begin{bmatrix} Z'_{11}c & Z'_{12}c & 0 \\ Z'_{21}c & Z'_{22}c & Z'_{23}c \\ 0 & Z'_{32}c & Z'_{33}c \end{bmatrix} \end{bmatrix} \tag{5.18}$$

with Z'_{ab}, Z'_{ac}, Z'_{bc} being the mutual impedances between the three outer loops of Fig. 5.8. By using Eq. (5.9) for the transformation from loop to phase (core, sheath, armor) quantities, the matrix in Eq. (5.18) becomes

$$[Z'_{phase}] = \begin{bmatrix} [Z'_{self-a}] & [Z'_{mutuala-b}] & [Z'_{mutuala-c}] \\ & [Z'_{self-b}] & [Z'_{mutualb-c}] \\ symmetric & & [Z'_{self-c}] \end{bmatrix} \tag{5.19}$$

The 3 x 3 submatrices $[Z_{self-a}]$ etc. on the diagonal are identical to the matrix in Eq. (5.10a) for each cable by itself, whereas the 3 x 3 off-diagonal matrices have identical elements, e.g.,

$$[Z'_{mutuala-b}] = \begin{bmatrix} Z'_{ab} & Z'_{ab} & Z'_{ab} \\ Z'_{ab} & Z'_{ab} & Z'_{ab} \\ Z'_{ab} & Z'_{ab} & Z'_{ab} \end{bmatrix} \tag{5.20}$$

The only elements not yet defined are the mutual impedances Z'_{ab}, Z'_{ab}, Z'_{bc} of the outer earth return loops, which are discussed in more detail in Section 5.3. If one of the cables does not have an armor, its self submatrix is obviously a 2 x 2 matrix and its mutual submatrix is a 2 x 3 matrix. For cables without sheath and armor, the submatrices become 1 x 1 and 1 x 3, respectively.

There is no coupling among the three phases in the shunt admittances. Therefore, the shunt admittance matrix for the three-phase system is simply

$$[Y'_{phase}] = \begin{bmatrix} [Y'_a] & 0 & 0 \\ 0 & [Y'_b] & 0 \\ 0 & 0 & [Y'_c] \end{bmatrix} \tag{5.21}$$

where $[Y'_a]$ is the 3 x 3 matrix of Eq. (5.17) for phase a, etc.

The screening effect of the sheath and armor depends very much on the method of grounding. For example, if cable a is operated at 100 A between core and ground, with sheath and armor ungrounded and open-circuited, then the full 100 A will flow in the outer loop (loop currents $I_1 = 100$, $I_2 = 100$, $I_3 = 100$ in Fig. 5.4). This will produce maximum induced voltages in the conductors of a neighboring cable b. How much nuisance this induction effect creates depends again on the method of grounding within cable b itself. If cable b is operated between core and ground (loads connected from core to ground), and if its sheath and armor are ungrounded and open-circuited, then the induced voltage will drive a circulating current through the core, ground and load impedances. If cable b is operated between core and sheath (loads connected from core to sheath), then there will be no circulating current in that loop, because according to Eq. (5.20), the induced voltages are identical in core and sheath. There would be a circulating current through the sheath and armor in parallel with earth return if the sheath (and armor) is grounded at both ends.

If both the sheath and armor in the current-carrying cable a are grounded at both ends, then the voltage induced in the conductors of the neighboring cable b would be small. For the practical example of a 500 kV ac

submarine cable at 60 Hz, 14% of the core current would return through the sheath, 87.8% through the armor, and only 5.6% through the outermost loop with ground or sea water return. The induction effect in neighboring cables would then be only 5.6% compared to the case with ungrounded sheath and armor. The algebraic sum is larger than 100% because there are phase shifts among the three currents ($I_{sheath} = 14e^{-j148^\circ}$, $I_{armor} = 87.8e^{+j179^\circ}$, $I_{earth} = 5.6e^{-j86^\circ}$).

5.3 Earth-Return Impedances[1]

In Eq. (5.4), the impedance of the loop formed by the outermost tubular conductor and the earth (or sea water) as return path is needed. This shall be called the "self earth-return impedance." For the matrix of Eq. (5.18), the "mutual earth-return impedance" Z'_{ik} between the loop formed by the outermost tubular conductor and the earth return path of cable i, and the analogous loop of cable k, is needed as well.

The four main methods of installing cables are as follows [148]:

(a) The cable is laid directly in the soil, in a trench which is filled with a backfill consisting of either the original soil or of other material with lower or more stable thermal resistivity.

(b) The cable is laid in ducts or troughs, usually of earthenware or concrete.

(c) The cable is drawn into circular ducts or pipes, which allows additional cables to be installed without excavation.

(d) The cable is installed, in air, e.g. in tunnels built for other purposes.

In cases (a), (b) and (c) the cable is clearly buried underground, and formulas for buried conductors must therefore be used. In case (a), the radius R of the outermost insulation is simply the outside radius of the cable. In cases (b) and (c) it should be the inside radius of the duct if the duct has a similar resistivity as the soil, or the outside radius if it is a very bad conductor, or possibly some average radius if it is neither a good nor a bad conductor. What to do in case (d) is somewhat unclear. Reasonable answers might be obtained by representing the tunnel with an equivalent circular cross section of radius R. Another alternative is to assume that the tunnel floor is the surface of the earth, and then use the earth-return impedance formula for overhead conductors. This would ignore current flows in the earth above the tunnel floor.

5.3.1 Buried Conductors in Semi-Infinite Earth

Exact formulas for the self and mutual earth-return impedances of buried conductors were first derived by Pallaczek [29]. In these formulas, the earth is treated as semi-infinite, extending from the surface downwards and sideways to infinity. If the horizontal distance between cable i and cable k is x, and if cable i and k are buried at depth h and y, respectively (Fig. 5.9), then the mutual earth-return impedance is [150]

$$Z'_{mutual} = \frac{\rho m^2}{2\pi}\{K_0(md) - K_0(mD) + \int_{-\infty}^{\infty} \frac{\exp\{-(h+y)\sqrt{\alpha^2+m^2}}{|\alpha| + \sqrt{\alpha^2+m^2}} \exp(j\alpha x)\, d\alpha\} \tag{5.22}$$

[1]The assistance of N. Srivallipuranandan and L. Marti in research for this section is gratefully acknowledged.

where

$d = \sqrt{x^2+(h-y)^2}$ = direct distance between cables i and k,

$D = \sqrt{x^2+(h+y)^2}$ = distance between cable i and image of cable k in air,

m = reciprocal of depth of penetration for earth from Eq. (5.7e),

α = integration constant.

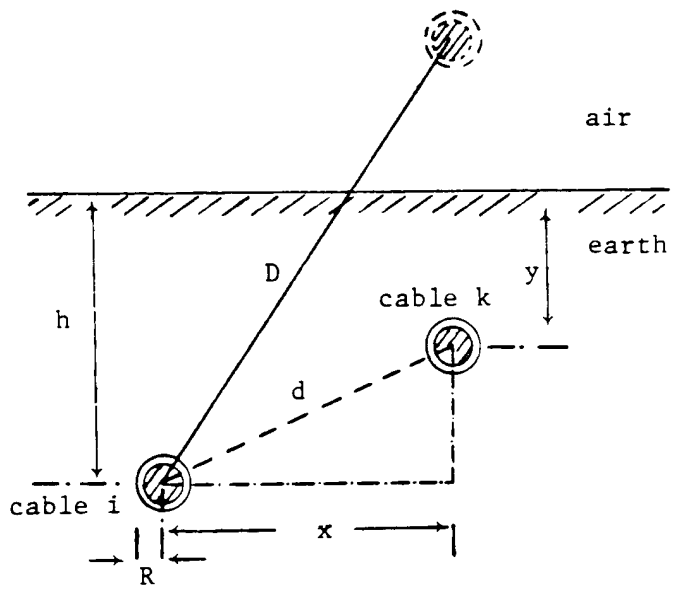

Fig. 5.9 - Geometric configuration of two cables

The self earth-return impedance is obtained from Eq. (5.22) by choosing the x,y- coordinate on the surface of the outermost insulation, e.g., x = R and y = H,

$$Z'_{earth} = \text{(same as Eq. (5.22), with } y = h,\ x = R) \tag{5.23}$$

with R = outside radius of outermost insulation. The permeability μ of earth and air are assumed to be identical in these equations. Furthermore, they are written in a slightly different form than in Pollaczek's original paper, but they are in fact identical.

While the K_0 terms in Eq. (5.22) are easy to evaluate, the integral terms in both (5.22) and (5.23) cannot be calculated that easily. Wedepohl [150] gives an infinite series, which has been compared by Srivallipuranandan [168] with a direct numerical integration method based on Romberg extrapolation. Both results agreed to within 0.1%. Since the function under the integral is highly oscillatory, direct numerical integration is not easy, and the series expansion is therefore the preferred approach.

The support routine CABLE CONSTANTS does not use the exact Pollaczek formula. Ametani recognized that the integral terms in Eq. (5.22) and (5.23) become identical with Carson's earth return impedance if the numerator $\exp\{-(h+y)\sqrt{\alpha^2+m^2}\}$ is replaced by $\exp\{-(h+y)|\alpha|\}$. Accepting this approximation, which is valid for $|\alpha| >> |m|$, he can then use Carson's infinite series or asymptotic expansion discussed in Section 4.1.1.1. Fig.

5.10 and 5.11 show the errors in Ametani's results from support routine CABLE CONSTANTS, as well as the errors of Wedepohl's approximate formulas [150] for self impedance,

$$Z'_{earth} = \frac{\rho m^2}{2\pi}\{-\ln\frac{\gamma mR}{2} + 0.5 - \frac{4}{3}mh\} \tag{5.24}$$

and for mutual impedance

$$Z'_{mutual} = \frac{\rho m^2}{2\pi}\{-\ln\frac{\gamma md}{2} + 0.5 - \frac{2}{3}m\mathcal{L}\} \tag{5.25}$$

with γ = Euler's constant, and

$\mathcal{L}$ = sum of the depths of burial of the two conductors.

Wedepohl's approximations are amazingly accurate up to 100 kHz (error < 1%), and then become less accurate as the frequency increases (25% error at 1 mHz) where the condition |mR| < 0.25 or |md| < 0.25 is no longer fulfilled.

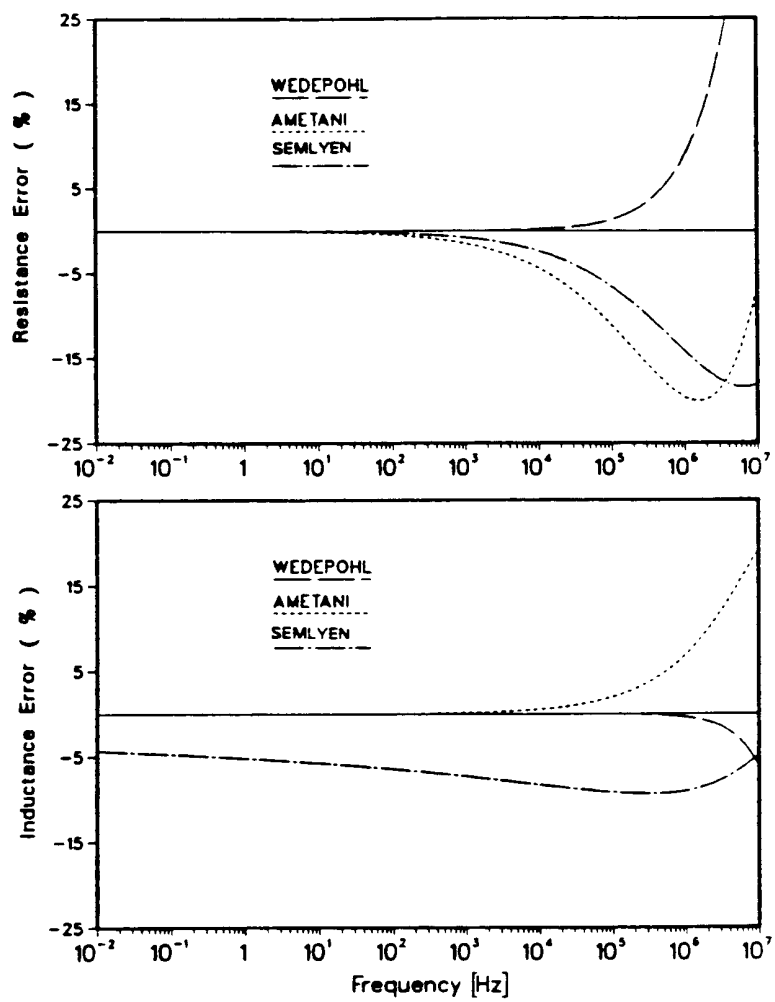

Fig. 5.10 - Relative errors in self earth-return impedance formulas for buried conductors (R = 48.4 mm, ρ = 100 Ωm) [168]. Reprinted by permission of N. Srivallipuranandan

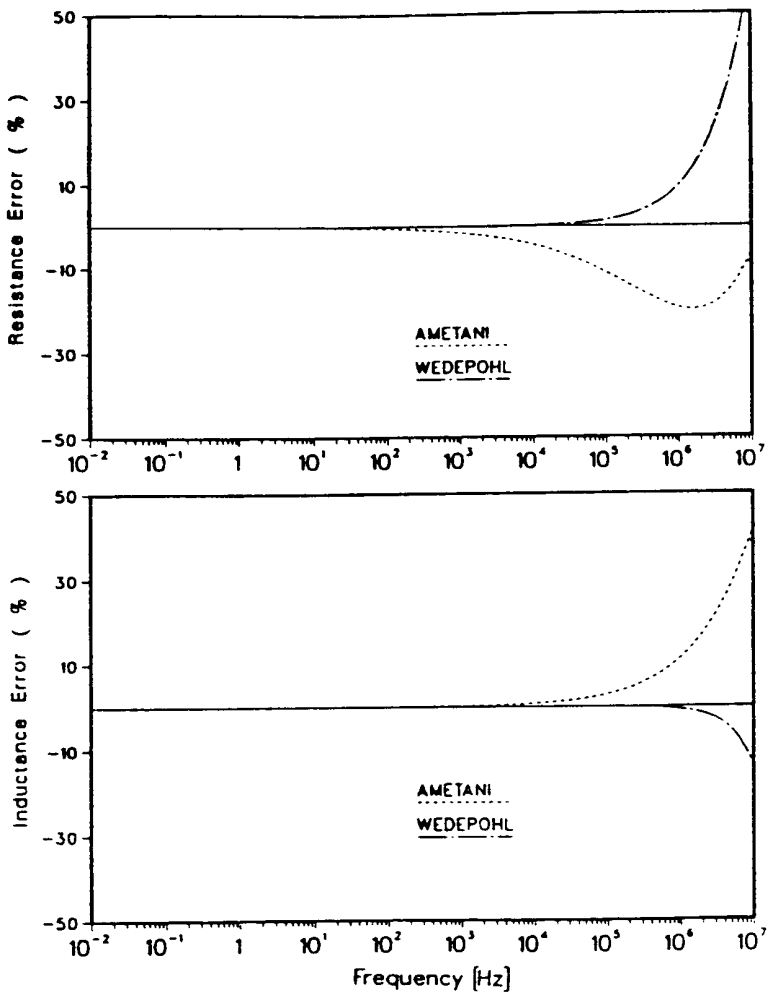

Fig. 5.11 - Relative error in mutual earth-return impedance formulas for buried conductors (d = 0.3 m, h = 0.75 m, y = 0.75 m) [168]. Reprinted by permission of N. Srivallipuranandan

Semlyen has recently developed a very simple formula based on complex depth (OVERLINE) p = 1/m [156], analogous to Eq. (4.3) for the case of overhead lines. For the self earth-return impedance, the formula is

$$Z'_{earth} = \frac{j\omega\mu}{2\pi} \ln(R + \frac{1}{mR}) \tag{5.26}$$

while a similar formula for the mutual impedance has not yet been found. The error of Eq. (5.26) is plotted in Fig. 5.10. Considering the extreme simplicity of this formula as compared to Pollaczek's formula, it is amazing to see how reasonable the results from this approximate formula are.

5.3.2 Buried Conductors in Infinite Earth

In some cases, it may be reasonable to assume that the earth is infinite in all directions around the cable. This assumption can be made when the depth of penetration in the earth

$$d_{earth} = \frac{\sqrt{2}}{|m|} = 503\sqrt{\frac{\rho_{earth(\Omega m)}}{f(Hz)}} \quad (m) \tag{5.27}$$

becomes much smaller than the depth of the burial. For submarine cables, where ρ is typically 0.2 Ωm, this is probably more or less true over the entire frequency range of interest, whereas for underground cables it would only be true above a few MHz or so. Bianchi and Luoni [151] have used this infinite earth assumption to find the sea return impedance of submarine cables.

The self earth-return impedance for infinite earth is easily obtained from the tubular conductor formula (5.7a), by letting the outside radius r go to infinity. Then with q = R,

$$Z'_{earth} = \frac{\rho m}{2\pi R}\frac{K_0(mr)}{K_1(mR)} \tag{5.28}$$

The mutual earth-return impedance was derived in [168] as

$$Z'_{mutual} = \frac{\rho\, K_0(md)}{2\pi R_i R_k K_1(mR_i)\, K_1(mR_k)} \tag{5.29}$$

5.3.3 Overhead Conductors

If the cable is installed in air, or laid on the surface of the ground, then the earth-return impedances are the same as those discussed for overhead lines in Section 4. The support routine CABLE CONSTANTS uses Carson's formula in that case. For a cable laid on the surface of the ground, the height is equal to R. Ametani has tried a special formula of Sunde for conductors on the surface of the ground, but the answers were found to be very oscillatory around the seemingly correct answer. Sunde's formula was therefore not implemented.

5.3.4 Mutual Impedance Between Overhead Conductor and Buried Conductor

There is inductive coupling between the loop of an overhead conductor with earth return and the loop of a buried conductor with earth return. The mutual impedance between these two loops is needed, for example, for studying the coupling effects in pipelines from overhead lines, as discussed in Section 5.6. This case was treated by Pollaczek as well, with

$$Z'_{mutual} = \int_{-\infty}^{\infty} \frac{\exp\{-h|\alpha| - y\sqrt{\alpha^2+m^2}\}}{|\alpha| + \sqrt{\alpha^2+m^2}} \exp(j\alpha x)\, d\alpha \tag{5.30}$$

As in the case of buried conductors, Ametani uses an approximation for this integral by replacing $y\sqrt{\alpha^2+m^2}$ with $y|\alpha|$. With this approximation, the formula becomes identical with Carson's equations, with the height of the buried conductor having a negative value. In connection with a pipeline study [158], it was verified that Carson's formula and Pollaczek's formula give identical results at 60 Hz. At higher frequencies, the differences would probably be similar to those shown in Fig. 5.11.

5.4 Pipe-Type Cable

Compared to the geometry of the single-core cable of Fig. 5.4, the geometry of the pipe-type cable of Fig. 5.3 is more complicated. It is therefore more complicated to obtain the impedances of a pipe-type cable, mainly for two reasons,

(a) The single-core cables inside the pipe are not concentric with respect to the pipe.

(b) The steel pipe is magnetic, and subject to current-dependent saturation effects.

The analysis is somewhat simplified by the fact that the depth of penetration into the pipe is less than the pipe thickness at power frequency and above. At 60 Hz, it is 1.5 mm from Eq. (5.27), with typical values of $\rho = 0.2 \bullet 10^{-6}$ Ωm and $\mu_r = 400$, whereas a typical pipe thickness for a 230 kV cable is 6.4 mm. For transient studies with frequencies above power frequency, the pipe thickness can therefore be assumed to be infinite, or equivalently, the earth-return can be ignored. Table 5.2 shows the current returning in the earth for a single-phase-to-ground

Table 5.2 - Earth-return current in a 230 kV pipe-type cable for single-phase fault ($\mu_r = 400$)

f (Hz)	current in earth (percent of core current)
0.6	94.50
6	31.00
60	0.85
600	0.00

fault in a 230 kV pipe-type cable, with the pipe being in contact with the earth. To arrive at these values, it was assumed that the core of the faulted phase was in the center of the pipe, and that the two unfaulted phases can be ignored. With these assumptions, the impedance formulas of Section 5.1 can be used. If the two unfaulted phases were included, the earth-return current would probably be even less because some current would return through the shield tapes and skid wires of the unfaulted phases. The relative permeability μ_r influences the values of Table 5.2; with $\mu_r = 50$, 6% of the current would return through the earth at 60 Hz, or 0.02% with $\mu_r = 1600$.

5.4.1 Infinite Pipe Thickness (No Earth Return)

If the depth of penetration is less than the pipe thickness, then no voltage will be induced on the outside of the pipe ($Z'_{\text{pipe-mutual}} = 0$ from Eq. (5.7c)), and consequently, the loop current pipe/earth return will be practically zero. In that case, the pipe is the only return path. The configuration is then essentially the same as that of three single-core cables in Fig. 5.8, except that the pipe replaces the earth as the return path.

If we assume that each phase consists of three conductors (e.g., core, shield tapes represented as sheath, skid wires represented as armor), then the loop impedance matrix is the same as in Eq. (5.18). Coupling will only exist among the three outermost loops of each armor (skid wires) with return through the pipe. What is needed then

is a formula for the self impedances Z'_{33a}, Z'_{33b}, Z'_{33c} of the loops formed by each armor (skid wires) and the pipe, and a formula for the mutual impedances Z'_{ab}, Z'_{bc}, Z'_{ca} between two such loops.

The support routine CABLE CONSTANTS finds these impedances with formulas first derived by Tegopoulos and Kriezis [159], and later used by Brown and Rocamora [160]. In these formulas it is assumed that the current is concentrated in an infinitesimally small filament at the center of each single-core cable. This model can be applied to conductors of finite radius if proximity effects are negligible, either because of symmetrical positioning within the pipe, or because the conductor radius is small compared to the distance to other conductors or the pipe wall. In pipe-type cables, neither condition is met since the conductors are relatively large and lie on the bottom of the pipe. The pipe-type cable impedances from CABLE CONSTANTS are therefore not completely accurate, but no better analytical models are available at this time. Brown and Rocamora, who proposed the formulas originally, recommend methods based on the subdivision into partial conductors discussed in Section 5.7, for more accurate impedance calculation [161]. Hopefully, a support routine based on the subdivision method will become available some day.

The self impedance Z'_{33a}, etc. of the loop between the armor (skid wires) and the pipe consists again of three terms, as in Eq. (5.4). The first term $Z'_{\text{armor-out}}$ is the same as in Eq. (5.7b), with the assumption that proximity effects can be ignored. The second term for the insulation becomes more complicated than Eq. (5.6), because of the eccentric geometry,

$$Z'_{insulation} = j\omega \frac{\mu_0}{2\pi} \ln\left\{\frac{q}{R_i}\left[1 - \left(\frac{d_i}{q}\right)^2\right]\right\} \tag{5.31}$$

with q, R_i and d_i defined in Fig. 5.12. The third term for the internal impedance of the pipe, with return on the inside, replaces Z'_{earth} in Eq. (5.4):

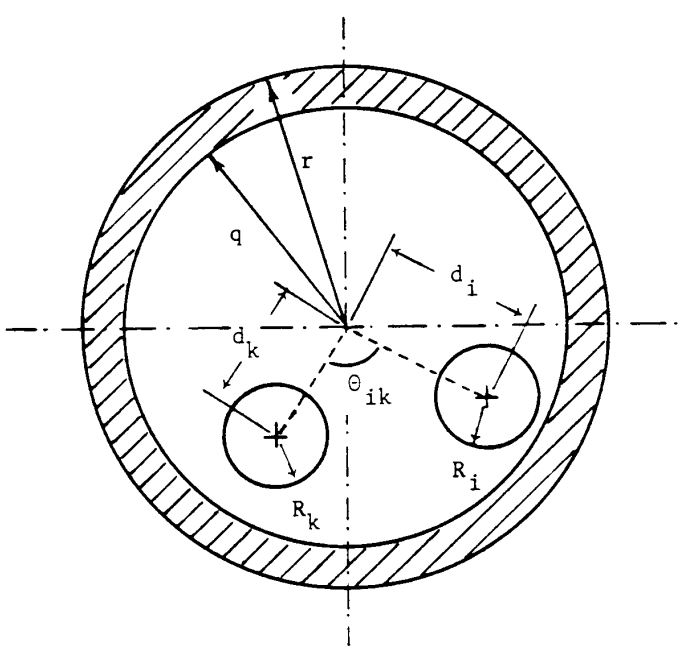

Fig. 5.12 - Geometry of pipe-type cable (q,r = inside and outside radius of pipe; R_i, R_k = outside radius of single-core cables i, k; d_i, d_k = offset from center)

$$Z'_{pipe\text{-}in} = j\omega\frac{\mu}{2\pi}\left\{\frac{K_0(mq)}{mqK_1(mq)} + 2\sum_{n=1}^{\infty}\left(\frac{d_i}{q}\right)^{2n}\frac{K_n(mq)}{n\mu_r K_n(mq) - mqK'_n(mq)}\right\} \tag{5.32}$$

with m from Eq. (5.7e), and $\mu = \mu_0\mu_r$ = permeability of the pipe,

K_i = modified Bessel function of the second kind of order i

K'_i = derivative of K_i.

For the concentric case with $d_i = 0$, Eq. (5.32) becomes identical with Eq. (5.28).

The mutual impedance Z'_{ab}, etc. between two outermost loops formed by armor (skid wires) and pipe is

$$Z'_{mutual} = j\omega\frac{\mu_0}{2\pi}\{\ln\frac{q}{\sqrt{d_i^2 + d_k^2 - 2d_i d_k\cos\Theta_{ik}}} + \mu_r\frac{K_0(mq)}{mqK_1(mq)}$$

$$+ \sum_{n=1}^{\infty}(\frac{d_i d_k}{q^2})^n\cos(n\Theta_{ik})(2\mu r\frac{K_n(mq)}{n\mu_r K_n(mq) - mqK'_n(mq)} - \frac{1}{n})\} \tag{5.33}$$

Except for replacing Z'_{earth} with $Z'_{pipe\text{-}in}$, and for using Z'_{mutual} from Eq. (5.33) instead of (5.22), all calculations remain the same as in Section 5.2, including the transformation from loop to phase quantities. If the cables inside the pipe do not have an armor (skid wires) or a sheath (shield tapes), then some of the matrices will be reduced to 2 x 2, or 1 x 1, as discussed in Section 5.2. In practice, the shield tapes and skid wires can probably be represented as one single sheath.

The magnetic properties of the steel pipe are easily taken into account by using the proper values for the relative permeability μ_r in Eq. (5.32) and (5.33). Unfortunately, μ_r depends on the current because of saturation effects, as shown in Fig. 5.13 [192]. To model saturation effects accurately is not simple, because even at one frequency, say at 60 Hz, the permeability would not remain constant over one cycle. A two-slope saturation curve was tried in [161], with the conclusion that reasonably accurate answers can be obtained with a constant value of μ_r. The sensitivity of the results with respect to μ_r can then be checked by re-running the case with one or more different values of μ_r.

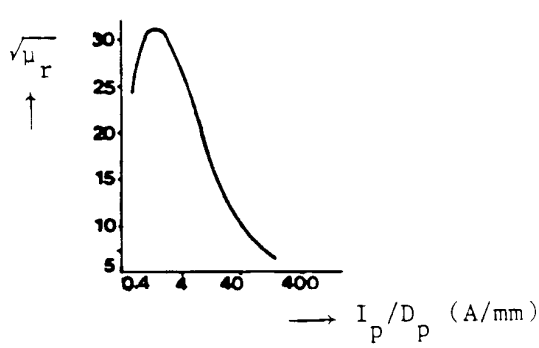

Fig. 5.13 - Relative permeability as a function of pipe current (I_p = pipe current, D_p = pipe diameter) [192]. © 1964 IEEE

Since the shield tapes and skid wires are in contact with the pipe wall, the values of the capacitances between the shield tapes/ skid wires of the three phases and between them and the pipe are immaterial. They are shorted out. Eq. (5.21) can therefore be used directly for the shunt admittance matrix. The support routine CABLE CONSTANTS does not assume this contact with the pipe in the beginning, however, and is therefore more general. For this general case, a potential coefficient matrix is found first,

$$[P'_{phase}] = \begin{bmatrix} [P'_a] & & \\ & [P'_b] & \\ & & [P'_c] \end{bmatrix} + \begin{bmatrix} [P'_{aa}] & [P'_{ab}] & [P'_{ac}] \\ P'_{ba}] & [P'_{bb}] & [P'_{bc}] \\ [P'_{ca}] & [P'_{cb}] & [P'_{cc}] \end{bmatrix} \tag{5.34}$$

where $[P'_a]$, $[P'_b]$, $[P'_c]$ are the 3 x 3 matrices of each single-core cable found by inversion of Eq. (5.17) with G' = 0,

$$[P'_a] = \begin{bmatrix} C'_1 & -C'_1 & 0 \\ -C'_1 & C'_1+C'_2 & -C'_2 \\ 0 & -C'_2 & C'_2+C'_3 \end{bmatrix}^{-1} \tag{5.35a}$$

or [163]

$$[P_a'] = \begin{bmatrix} P'_1+P'_2+P'_3 & P'_2+P'_3 & P_3 \\ P'_2+P'_3 & P'_2+P'_3 & P'_3 \\ P'_3 & P'_3 & P'_3 \end{bmatrix} \tag{5.35b}$$

with $P_i' = 1/C_i'$. (5.35c)

The dielectric between the armors (skid wires) and the pipe is represented by the second term in Eq. (5.34). Each of the submatrices $[P_{ii}']$ and $[P_{ik}']$ in the second term is a 3 x 3 matrix with 9 equal elements,

$$P_{ii}' = \frac{1}{2\pi\varepsilon_0\varepsilon_r} \ln\left\{\frac{q}{R_i}\left[1 - \left(\frac{d_i}{q}\right)^2\right]\right\} \tag{5.36a}$$

$$P_{ik}' = \frac{1}{2\pi\varepsilon_0\varepsilon_r} \ln \frac{q}{\sqrt{d_i^2 + d_k^2 - 2d_i d_k \cos\Theta_{ik}}} \tag{5.36b}$$

with the essential terms in Eq. (5.36) being the same expressions appearing in Eq. (5.31) and (5.33). The admittance matrix is then found by inverting $[P'_{phase}]$,

$$[Y'_{phase}] = j\omega[P'_{phase}]^{-1} \tag{5.37}$$

5.4.2 Finite Pipe Thickness with Earth Return

At lower frequencies, there is mutual coupling between the inner and outer surface of the pipe. The induced voltage on the outer surface will then produce a circulating current through the pipe and earth return. This extra loop must be added to the loop impedance matrix of Eq. (5.18),

$$[Z'_{loop}] = \left[\begin{array}{c|c} \text{as in Eq. (5.18),} & 0 \\ \text{with elements defined} & 0 \\ \text{in Section 5.4.1} & -Z'_m \\ & 0 \\ & 0 \\ & -Z'_m \\ & 0 \\ & 0 \\ & -Z'_m \\ \hline 0\ 0\ -Z'_m\ 0\ 0\ -Z'_m\ 0\ 0\ -Z'_m & Z'_s \end{array}\right] \tag{5.38a}$$

with

$$Z'_m = Z'_{pipe\text{-}mutual} \text{ from Eq. (5.7c),} \tag{5.38b}$$

$$Z'_s = Z'_{pipe\text{-}out} + Z'_{insulation} + Z'_{earth}. \tag{5.38c}$$

The first two terms in Eq. (5.38c) are found from Eq. (5.7b) and (5.6) ($Z'_{insulation} = 0$ if pipe in contact with earth), and Z'_{earth} is the earth-return impedance discussed in Section 5.3. Transforming Eq. (5.38a) to phase quantities produces

$$[Z'_{phase}] = \left[\begin{array}{c|c} \text{same matrix as} & 0 \\ \text{for infinite} & 0 \\ \text{pipe thickness} & . \\ & . \\ & \\ 0\ 0\ \ldots & 0 \end{array}\right] \left[\begin{array}{c|c} Z'\ Z'\ \ldots Z' & Z'_e \\ Z'\ Z'\ \ldots Z' & Z'_e \\ \ldots\ldots\ldots\ldots & . \\ \ldots\ldots\ldots\ldots & . \\ Z'\ Z'\ \ldots Z' & Z'_e \\ \hline Z'_e\ Z'_e\ \ldots Z'_e & Z'_s \end{array}\right] \tag{5.39a}$$

with Z_s' from Eq. (5.38c)

$$Z_e' = Z_s' - Z_m' \tag{5.39b}$$

$$Z' = Z_s' - 2Z_m'$$

The last row and column in Eq. (5.39a) represent the pipe quantities, while the first 9 rows and columns refer to core, sheath (shield tapes), armor (skid wires) of phases a, b, and c.

If the pipe is in contact with the earth, then the shunt admittance matrix is the same as in Section 5.4.1. If it is insulated, then the potential coefficient matrix of Eq. (5.34) must be expanded with one extra row and column for the pipe, and the same element

$$P' = \frac{1}{2\pi\varepsilon_0\varepsilon_r}\ln\frac{r_{pipe-insulation}}{r_{pipe-outside}} \tag{5.40}$$

must be added to this expanded matrix,

$$[P'_{phase}] = \left[\begin{array}{c|c} \text{same as in} & 0 \\ \text{Eq. (5.34)} & 0 \\ & . \\ & . \\ 0\ 0\ \ldots & 0 \end{array}\right] + \begin{bmatrix} P'\ P' & \ldots P' \\ P'\ P' & \ldots P' \\ \ldots & \ldots \\ P'\ P' & \ldots P' \end{bmatrix} \tag{5.41}$$

The admittance matrix is then again found by inversion with Eq. (5.37).

5.5 Building of Conductors and Elimination of Grounded Conductors

Conductors are sometimes connected together ("bundled"). For example, the concentric neutral conductors in the cable of Fig. 5.2 are in contact with each other, and therefore electrically connected. In a pipe-type cable, the shield tapes and skid wires are in contact with the pipe. In a submarine cable, the sheath is often bonded to the armor at certain intervals, to avoid voltage differences between the sheath and armor.

In such cases, the connected conductors 1,...m can be replaced by (or bundled into) one equivalent conductor, by introducing the bundling conditions

$$I_1 + I_2 + \ldots I_m = I_{equiv};\ V_1 = V_2 = \ldots V_m = V_{equiv} \tag{5.42}$$

into the equations for the series impedance and shunt admittance matrices. The bundling procedure for reducing the equations from m individual to one equivalent conductor is the same as Method 1 of Section 4.1.2.2 for overhead lines, and is therefore not explained again. It is exact if the conductors are continuously connected with zero connection resistance (as the neutral conductors in Fig. 5.2), and accurate enough if the connections are made at discrete points with negligible resistance (as in bonding of the sheath to the armor), as long as the distance between the connection points is short compared to the wavelength of the highest frequency in the transient simulation.

As in the case of overhead lines with ground wires, some conductors in a cable may be grounded. For example, the steel pipe of a pipe-type cable can usually be assumed grounded, because its asphalt mastic coating is not an electric insulation. Also, neutral conductors may be connected to ground at certain intervals, or at both ends. If a conductor i is grounded, then the condition is simply

$$V_i = 0 \tag{5.43}$$

and conductor i can then be eliminated from the system of equations in the same way as described in Section 4.1.2.1. Again, the elimination is only exact if the conductor is grounded continuously with zero grounding resistance, and accurate enough if the distance between discrete grounding points is short compared to the wavelength of the highest frequency.

An example of bundled as well as grounded conductors would be a single-core submarine cable which has its sheath bonded to the armor. Since the asphalt coating of the armor is not an electric insulation, the armor is in effect

in contact with the sea water, and both sheath and armor are therefore grounded conductors. By eliminating both of them, the submarine cable can be represented by single-phase equations for the core conductor, with the current return combined in sea water, armor and sheath. For an overhead line, the equivalent situation would be a single-phase line with two ground wires.

The case of segmented ground wires in overhead lines discussed in Section 4.1.2.5(b) can exist in cables as well. For example, if the sheath is grounded at one end, but open and ungrounded at the other end, then the sheath could be eliminated in the same way as segmented ground wires, provided the cable length is short compared to the wavelength of the highest frequency. The support routine CABLE CONSTANTS does not have an option for such eliminations. The user must represent the sheath as an explicit conductor, instead, with one end connected to ground. This offers the advantage that the induced voltage at the other end can automatically be obtained, if so desired.

5.6 Buried Pipelines

Pipelines buried close to power lines can be subjected to hazardous induction effects, especially during single-line-to-ground faults. To study these effects, one can include the pipeline as an additional conductor into the transmission line representation (Fig. 5.14(a)). For steady-state analysis, one can also use the single-phase representation of Fig. 5.14(b), with an impressed voltage

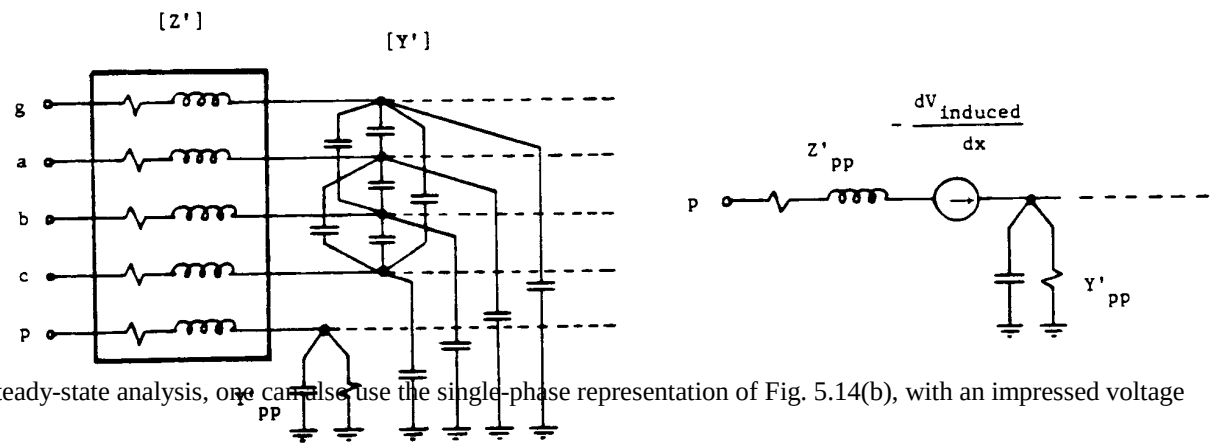

steady-state analysis, one can also use the single-phase representation of Fig. 5.14(b), with an impressed voltage

(a) polyphase representation (b) single-phase representation

Fig. 5.14 - Pipeline representation (g = ground wire, a, b, c = phase conductors, p = pipeline)

$$-\frac{dV_{induced}}{dx} = Z'_{pa}I_a + Z'_{pb}I_b + Z'_{pc}I_c + Z'_{pg}I_g \tag{5.44}$$

There is no capacitive coupling between the power line and the pipeline if it is buried in the ground.

As explained later, nominal π-circuits can only be used for very short lengths of pipeline (typically ≤ 0.3 km at 60 Hz). The single-phase representation is therefore preferable for steady-state analysis, because the distributed parameters of Fig. 5.14(b) are more easily converted into an exact equivalent π-circuit than the polyphase parameters of Fig. 5.14(a). This results in the active equivalent π-circuit of Fig. 5.15, with Y_{series} and Y_{shunt} being the usual

parameters obtained from Eq. (1.14), while $I_{induced}$ is an active current [158],

$$I_{induced} = \frac{-dV_{induced}/dx}{Z'_{pp}} \tag{5.45}$$

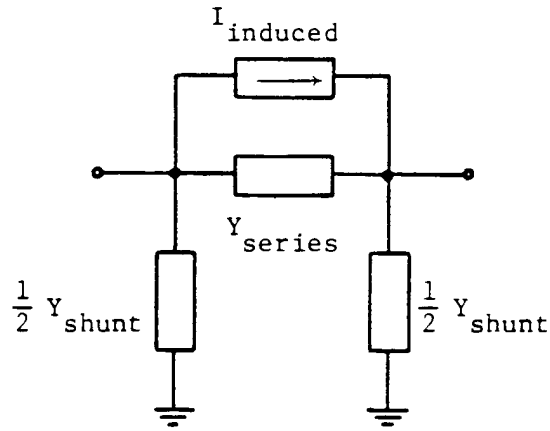

Fig. 5.15 - Active equivalent π-circuit

The correctness of the active π-circuit can easily be shown. Starting from the differential equations

$$-\frac{dV}{dx} = Z'_{pp} + Z'_{pp} I_{induced}$$

$$-\frac{dI}{dx} = Y'_{pp} V$$

the introduction of a modified current

$$I_{modified} = I + I_{induced}$$

transforms the differential equations into the normal form of the line equations, with the assumption that $I_{induced}$ does not change along the line ($dI_{modified}/dx = dI/dx$),

$$-\frac{dV}{dx} = Z'_{pp} I_{modified}$$
$$-\frac{dI_{modified}}{dx} = Y'_{pp} V$$

The solution for a line between nodes k and m is given in Eq. (1.13), except that the current is now $I_{modified}$, or rewritten,

$$\begin{bmatrix} I_{km} + I_{induced} \\ I_{mk} - I_{induced} \end{bmatrix} = \begin{bmatrix} Y_{series} + (1/2)Y_{shunt} & -Y_{series} \\ -Y_{series} & Y_{series} + (1/2)Y_{shunt} \end{bmatrix} \begin{bmatrix} V_k \\ V_m \end{bmatrix}$$

This is exactly the same equations which comes out of the equivalent circuit of Fig. 5.15.

With this single-phase approach, the currents in the power line are assumed to be known, e.g., from the usual type of short-circuit study. It is also assumed that they are constant over the length of the exposure to the pipeline, and that the pipeline runs parallel to the power line (mutual impedances constant). If either assumption is not true, then the power line-pipeline system must be split up into shorter sections as is customarily done in interference studies. The effect of the pipe on the power line zero sequence impedance is usually ignored, but could be taken into account.

In both representations of Fig. 5.14, the mutual impedances between the pipe and the overhead conductors, as well as the self impedance of the pipe with earth return, are needed. The mutual impedances are obtained with the formulas discussed in Section 5.3.4. At 60 Hz, Carson's formula will give practically identical results as the more complicated formula of Pollaczek.

The self impedance Z'_{pp} of the pipeline consists of the same three terms shown for the armor in Eq. (5.4). The first two terms are calculated with Eq. (5.7b) and (5.6), while R'_{earth} is found from the equations discussed in Section 5.3.

For the shunt admittance $Y'_{pp} = G' + j\omega C'$, the capacitive part is calculated in the usual way with Eq. (5.13). In contrast to the underground cable, the shunt conductance G' of the pipeline can no longer be ignored. The insulation around pipelines is electrically poor, either originally or because of puncturing during the laying operation. The loss angle δ in Eq. (5.14) is so large on pipelines insulated with glass-fiber/bitumen that G' becomes much larger than $\omega C'$ at power frequency, and if one part of the shunt admittance is ignored it should be $\omega C'$ rather than G'. On PVC-insulated pipelines, G' may still be smaller than $\omega C'$, though.

If the shunt resistance of the insulation is relatively small, then the grounding resistance of the pipe should be connected in series with it[2] [170], or

$$G' = \frac{1}{R'_{insulation} + R'_{grounding}} \tag{5.46}$$

where $R'_{insulation}$ = resistance of pipe insulation,

$R'_{grounding}$ = grounding resistance.

A useful formula for the grounding resistance is [170]

$$R'_{grounding} = \frac{\rho_{earth}}{4\pi}\left[2\ln\frac{2\mathcal{L}}{D} + \ln\frac{\sqrt{(2h)^2+\left(\frac{\mathcal{L}}{2}\right)^2}+\frac{\mathcal{L}}{2}}{\sqrt{(2h)^2+\left(\frac{\mathcal{L}}{2}\right)^2}-\frac{\mathcal{L}}{2}}\right] \tag{5.47}$$

with ρ_{earth} = earth resistivity (e.g., in Ωm),

h = depth of burial of pipe

$\mathcal{L}$ = length of pipe

---

[2]If the sheath, armor, or pipe of an underground cable or the ground wire of an overhead line is grounded, then it has been standard practice to ignore the grounding resistance (V = 0). An alternative would be to use a finite shunt admittance $Y' = 1/R'_{grounding}$, as recently suggested [186].

D = outside diameter of pipe.

Grounding grids must generally be analyzed as three-dimensional problems, even if they consist of only one pipe. The grounding resistance from Eq. (5.47) is therefore no longer an evenly distributed parameter, but depends on the length. Fortunately, the dependence of G' on length is very small for typical values of $G'_{insulation}$ [158]. In the region of measured values for G' between 0.1 S/km for newly-layed pipelines and 0.3 S/km for older pipelines with glass fiber/bitumen insulation [170], the dependence of G' on length is practically negligible, as shown in Fig. 5.16. Treating G' as an evenly distributed parameter is therefore a reasonable approximation.

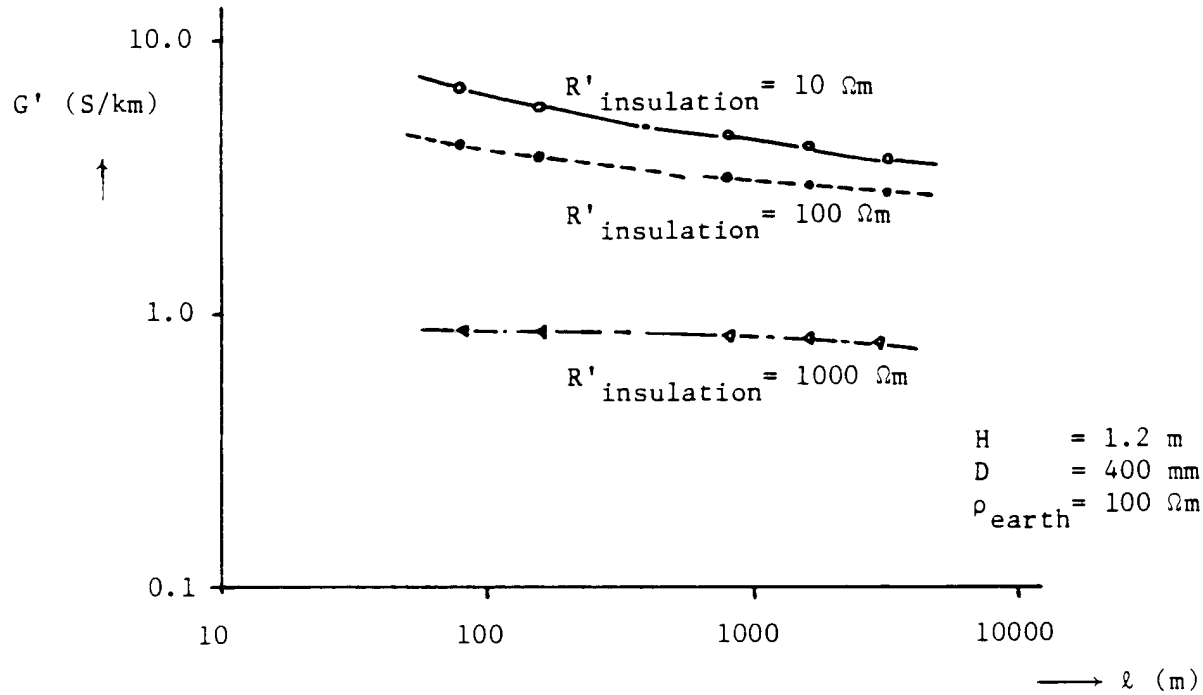

Fig. 5.16 - Shunt conductance of buried pipe

Because of G' >> ωC', the wavelength of buried pipelines is significantly shorter than that of underground cables, as shown in Table 5.3 [170]. Therefore, a nominal π-circuit of a circuit which includes a buried pipeline should not be longer than approximately 0.8 km for

Table 5.3 - Wavelength of pipeline at 50 Hz [170]

G' (S/km)	wavelength (km)
0.1	41.3
1.0	13.1
10.0	4.13

steady-state analysis, or approximately 0.08 km for switching surge studies [158].

Fig. 5.17 shows a comparison between measured and calculated voltages and currents in a pipeline, induced by currents in a neighboring power line, with the pipeline representation as discussed here [158].

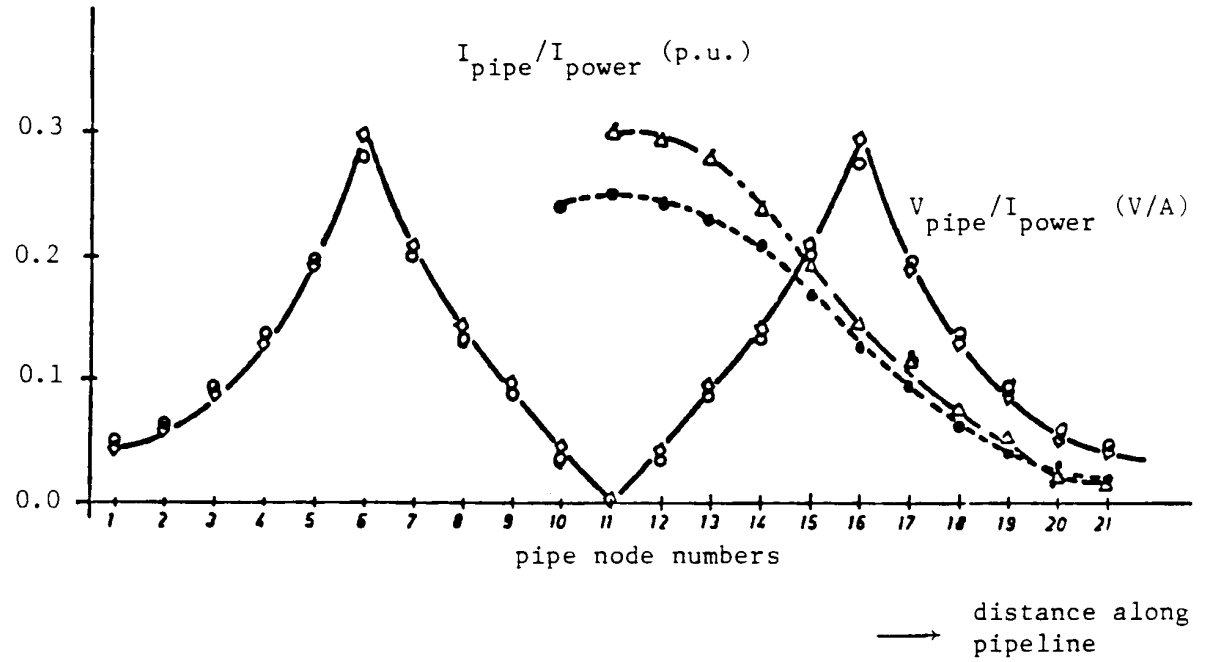

PIPE VOLTAGE

◊ Bücker measured
o calculated from single-phase π-model

PIPE CURRENT

Δ Bücker measured
● calculated from single-phase π-model

I_{power} = fault current in power line

Fig. 5.17 - Induced voltages and currents in a buried pipeline

5.7 Partial Conductor and Finite Element Methods

The support routine CABLE CONSTANTS uses analytical formulas which are essentially only applicable to configurations with axial symmetry. The formulas for the nonconcentric configuration in pipe-type cables (Section 5.5) are only approximate, and the authors of these formulas themselves suggest improvements along the lines discussed here.

To find the impedances and capacitances for conductor systems with arbitrary shapes (e.g., for the cable of Fig. 5.1), numerical methods can be used in place of analytical formulas, which are either based on subdivisions into partial conductors or on finite element methods. There is no support routine yet in the EMTP which uses these numerical methods. The principle of these methods is therefore only outlined very briefly.

5.7.1 Subdivision into Partial Conductors

With this method, each conductor is subdivided into small "partial" conductors ("subconductors" in [162], "segments" in [164]), as shown in Fig. 5.18. Various shapes can be used for the partial conductors, with rectangles being the preferred shape for strip lines in

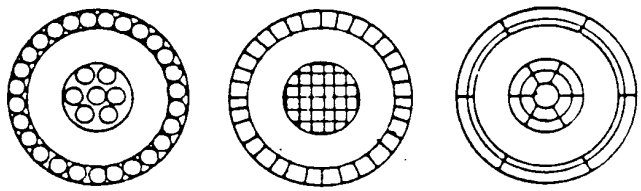

Fig. 5.18 - Subdivision of the main conductors into partial conductors

integrated circuits (Fig. 5.19).

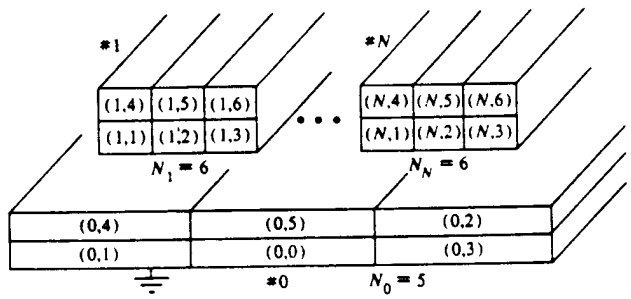

Fig. 5.19 - Subdivision of strip lines into partial conductors of rectangular shape [164]. Copyright 1979 by International Business Machines Corporation; reprinted by permission

In deriving the equations for the system of partial conductors, uniform current density is assumed within each partial conductor. Then the voltage drops along a system of n partial conductors at one frequency are described by the phasor equations

$$-\begin{bmatrix} dV_1/dx \\ dV_2/dx \\ \cdot \\ \cdot \\ dV_n/dx \end{bmatrix} = \left[\begin{bmatrix} R_1 & & & \\ & R_2 & & \\ & & \cdot & \\ & & & \cdot \\ & & & R_n \end{bmatrix} + j\omega \begin{bmatrix} L_{11} & L_{12} & \cdot & \cdot & L_{1n} \\ L_{21} & L_{22} & \cdot & \cdot & L_{2n} \\ \cdot & \cdot & \cdot & \cdot & \cdot \\ L_{n1} & L_{n2} & \cdot & \cdot & L_{nn} \end{bmatrix}\right] \begin{bmatrix} I_1 \\ I_2 \\ \cdot \\ \cdot \\ I_n \end{bmatrix} \tag{5.48}$$

The diagonal resistance matrix contains the dc resistances, and the full inductance matrix contains the self and mutual inductances of the partial conductors. The formulas for the matrix elements depend on the shape of the partial conductor, but they are well known.

To obtain the frequency-dependent impedance of a cable system, the matrices [R] and [L] are first computed. At each frequency, the complex matrix [Z] = [R] + jω[L] is formed, and reduced to the number of actual conductors with Bundling Method 1 of Section 5.5. For example, if partial conductors 1,...50 belong to the core conductor, and partial

conductors 51,...120 to the sheath, then this bundling procedure will reduce the 120 x 120-matrix to a 2 x 2-matrix, which produces the frequency-dependent impedances

$$\begin{bmatrix} Z_{cc}(\omega) & Z_{cs}(\omega) \\ Z_{cs}(\omega) & Z_{ss}(\omega) \end{bmatrix}.$$

This numerical method works well as long as the conductors are subdivided into sufficiently small partial conductors. The size of these partial conductors must be of the same order of magnitude as the depth of penetration.

5.7.2 Finite Element Methods

Finite element methods are more powerful than partial conductor methods in one sense, inasmuch as it is not necessary to assume uniform current density within each element. However, it is very difficult to handle open-boundary conditions with finite element methods, that is configurations where the magnetic field diminishes gradually as one moves away from the conductors, with no clearly defined boundary of known magnetic vector potential reasonably close to the conductors. In situations where a boundary is clearly defined, e.g., in pipe-type cables at high frequency where the depth of penetration becomes much less than the wall thickness, finite element methods can be quite useful.

With finite element methods, the region inside and outside of the conductors is subdivided into small elements, usually of triangular shape. Fig. 5.20(a) shows the example of a stranded conductor inside a pipe of radius R_b as the return path (clearly defined boundary with zero magnetic field A = 0 outside the pipe and zero derivative along the two edges of the "wedge"). Because of axial symmetry, it is sufficient to analyze the "wedge" shown in Fig. 5.20(a). This wedge region is then subdivided into triangular elements as shown in Fig. 5.20(b), with longer triangles as one moves away from the conductor.

The magnetic vector potential A is assumed to vary linearly along the edges and inside of each triangle,

$$A = ax + by + c, \tag{5.49}$$

when a first-order method is used (higher-order methods exist as well). The unknowns are essentially the values of A in the node points. If they were shown in the z-direction of a three-dimensional picture, then the triangles would appear in a shape similar to a geodesic dome, with the roof height being the value of A. The equations for finding A are linear algebraic

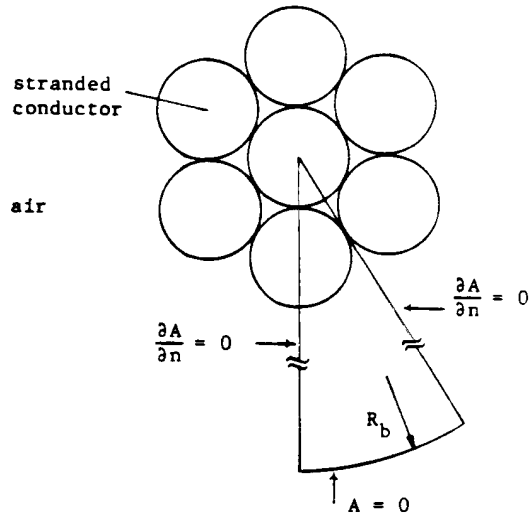

(a) Stranded conductor inside pipe of radius R_b

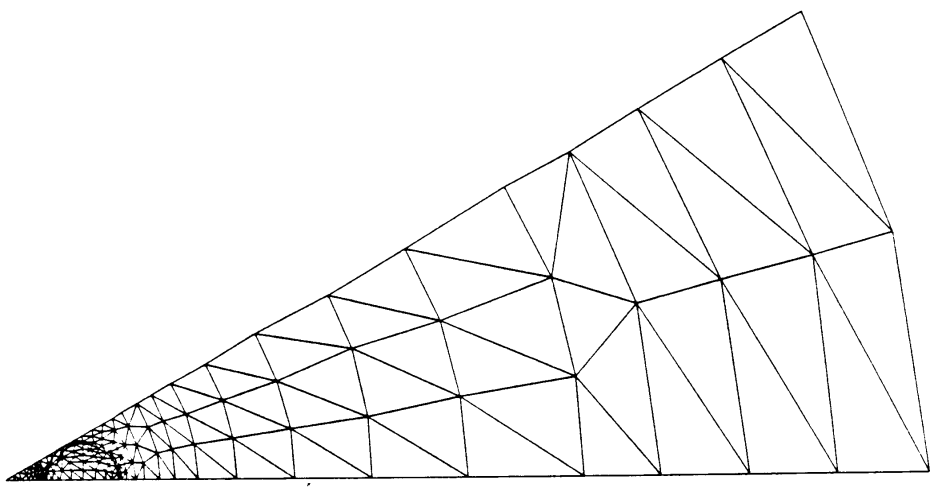

(b) Subdivision of region into triangular elements

Fig. 5.20 - Analysis of stranded conductor with finite element method [171]. Reprinted by permission of Yin Yanan

equations with a sparse matrix, but the number of node points or the number of equations is usually quite high (146 equations for the example of Fig. 5.20). Once the magnetic vector potential is known in the entire region, the impedances can be derived from it.

For readers interested in finite element methods for cable impedance calculations, the papers by Konrad, Weiss and Csendes [165, 166, 167] are a good introduction.

5.8 Modal Parameters

Once the series impedance and shunt admittance matrices per unit length $[Z'_{phase}]$, $[Y'_{phase}]$ are known, the derivation of modal parameters is exactly the same as described in Section 4.1.5 for overhead lines. They could be used, for example, to develop exact equivalent π-circuits for steady-state solutions as explained in Section 4.2.1.3.

For transient simulations, it is more difficult to use modal parameters, as compared to overhead lines, because the transformation matrix $[T_i]$ can no longer be assumed to be constant as for a single-circuit overhead line. Fig. 5.21 shows the variation of the elements in the third column of $[T_i]$ for a typical three-phase arrangement of 230 kV single-core cables with core conductor and sheath in each [155]. Especially around the power frequency of 50 or 60 Hz, the variations are quite pronounced.

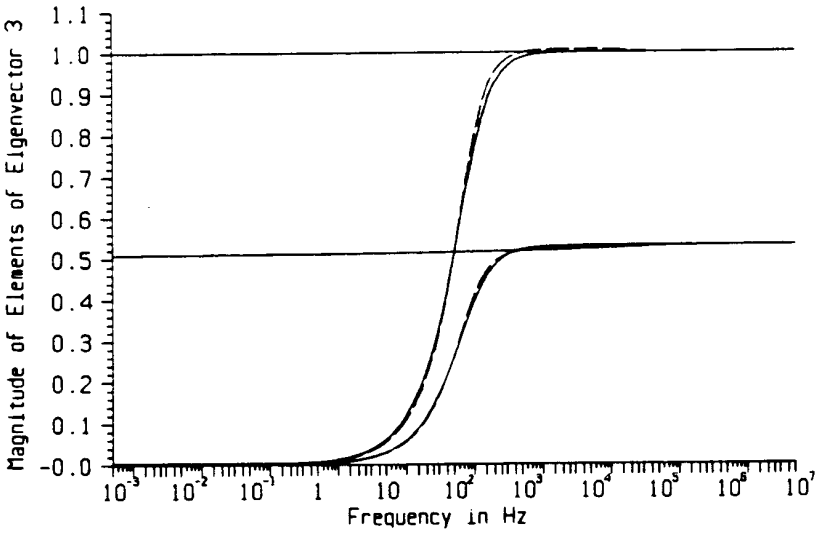

Fig. 5.21 - Magnitude of the elements of column 3 of $[T_i]$

Above a few kHz, the loop between core conductor and sheath becomes decoupled from the outer loop between sheath and earth return, because the depth of penetration on the inside of the sheath for loop 1 becomes much smaller than the sheath thickness. In that case, $Z_{\text{tube-mutual}} \sim 0$. This makes the transformation matrix constant above a few kHz, as evident from Fig. 5.21. For a single-phase single-core cable with sheath and armor, the three modes are identical with the 3 loops described in Eq. (5.1) at high frequency where $Z'_{12} \sim 0$ and $Z'_{23} \sim 0$. The transformation matrix between loop and phase quantities of Eq. (5.9),

$$[T_i]^{-1} = \begin{bmatrix} 1 & 0 & 0 \\ 1 & 1 & 0 \\ 1 & 1 & 1 \end{bmatrix} \quad and \quad [T_i] = \begin{bmatrix} 1 & 0 & 0 \\ -1 & 1 & 0 \\ 0 & -1 & 1 \end{bmatrix} \tag{5.50}$$

5.9 Cable Models in the EMTP

Co-author: L. Marti

As of now (Summer 1986), there are no specific cable models in the BPA EMTP. The only way to simulate cables is to fit cable data into the models available for overhead lines. It has long been recognized, of course, that this is only possible in a limited number of cases. A method specifically developed for cables, as discussed in Section 5.9.2.3, will hopefully be implemented in late 1986 or early 1987. It has already been tested extensively in the UBC

EMTP.

5.9.1 Ac Steady-State Solutions

In principle, there is no difficulty in representing cables as nominal or equivalent π-circuits in the same way as overhead lines (Section 4.2.1). If nominal π-circuits are used, it should be realized that the wavelength of underground cables is shorter than on overhead lines. If a nominal π-circuit should not be longer than 100 km at 60 Hz for overhead lines, the limit is more typically 30 km for underground cables. If a pipeline is modelled, the limit can be as low as 1 km, as discussed in Section 5.6.

Underground cables are often very short compared to the length of connected overhead lines. In such cases, the (complicated) series impedances have very little effect on the results because the system sees the cable essentially as a shunt capacitance. The cable can then be modelled as a simple lumped capacitance.

5.9.2 Transient Solutions

The accurate representation of cables with frequency-dependent impedances and frequency-dependent transformation matrices is discussed in Section 5.9.2.3. Situations where simpler models should be accurate enough are discussed first.

5.9.2.1 Short Cables

If a rectangular wave pulse travels on an overhead line and hits a relatively short underground cable, then the cable termination is essentially seen as a lumped capacitance. The voltage then builds up exponentially with a time constant of $T = Z_{overhead} \cdot C_{cable}$, shown in Fig. 5.22(a). If the cable is modelled somewhat more accurately as a lossless distributed-parameter line, then the voltage build-up has the staircase shape of Fig. 5.22(b), with the average of the sending and receiving end curve being more or less the same as the continuous curve in Fig. 5.22(a). As long as the travel time [] of the cable is short compared to the time constant T, reasonably accurate results can be obtained if the cable is represented as a lumped capacitance.

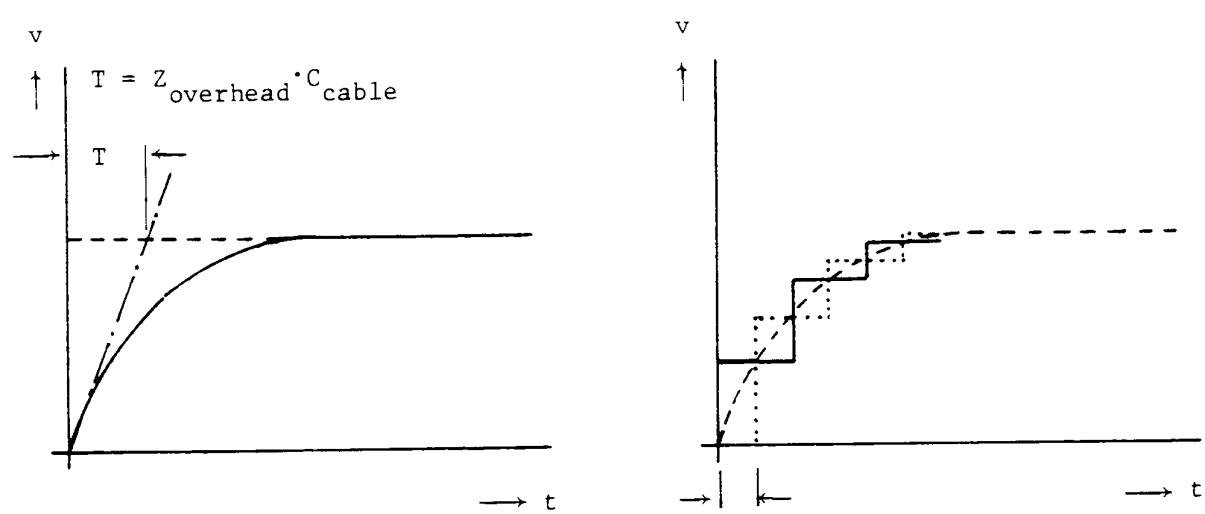

(a) Cable represented as lumped (b) Cable represented as

capacitance

lossless transmission line
------ sending end of cable
..... receiving end of cable

Fig. 5.22 - Voltage build-up in a cable connected to an overhead line

Nominal π-circuit representations have often been suggested as approximate cable models. They obviously represent the capacitance effect correctly, but the pronounced frequency-dependence in the series impedance is ignored. Nominal π-circuits give reasonable answers probably only in those cases in which the simpler lumped capacitance representation is already accurate enough.

5.9.2.2 Single-Phase Cables

There are situations where single-phase representations are possible. An example is a single-phase submarine cable in which the sheath and armor are bonded together, with the armor being in contact with the sea water. In such a case, the sheath and armor can be eliminated from Eq. (5.10), which results in the reduced single-phase equation

$$-\frac{dV_c}{dx} = Z'_{core} I_c$$

with Z'_{core} being the impedance of the core conductor with combined current return through sheath, armor and sea water. Coupling to the cables of the other two phases can be ignored because the three cables are layed relatively far apart, to reduce the risk of anchors damaging more than one phase in the same mishap.

When the equations have been reduced to single-phase equations, then it is straightforward to use the frequency-dependent overhead line model described in Section 4.2.2.6.

Sometimes it is not necessary to take the frequency-dependence in the series impedances into account. For example, single phase SF_6-busses have been modelled quite successfully for fast transients with two decoupled lossless single-phase lines, one for the inside coaxial loop and a second one for the outside loop between the enclosure and the earth-return. The coupling between the two loops through the enclosure is negligible at high frequencies because the depth of penetration is much less than the enclosure wall thickness. The only coupling occurs through reflections at the terminations. Agreement between simulation results from such simple models and field tests has been excellent [169].

5.9.2.3 Polyphase Cables [155]

The simple overhead line models with constant parameters discussed in Section 4.2.2 are of limited use for underground cables for two reasons:

(a) The transformation matrix $[T_i]$ is frequency-dependent up to a few kHz, though a constant $[T_i]$ would be acceptable for transients which contain only high frequencies (e.g., lightning surge studies).

(b) The modal parameters (e.g., wave velocity and attenuation) are more frequency-dependent than on overhead lines, as shown in Fig. 5.23 for three single-core cables with core and sheath [150].

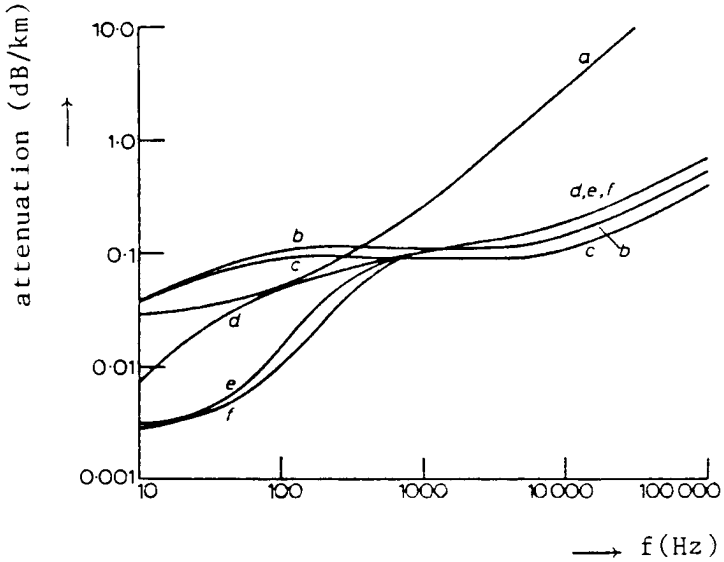

(a) Attenuation

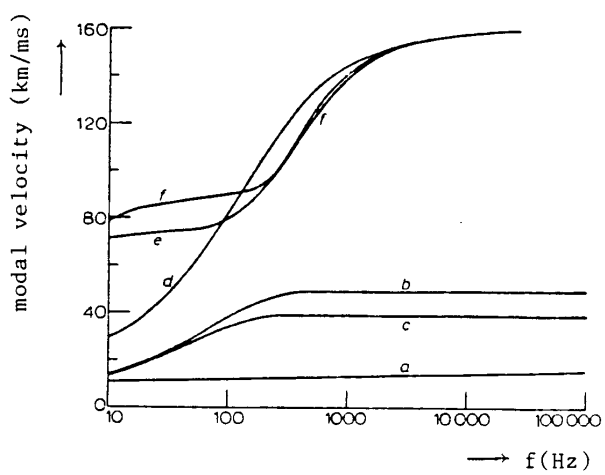

(b) Velocity

Fig. 5.23 - Modal parameters as a function of frequency [150]. Reprinted by permission of IEE and the authors

To derive an accurate model for an n-conductor cable system between nodes k and m, we can start from the phasor equation (4.121) for the overhead line, if we replace that scalar equation, which was written for one phase or mode, by a matrix equation for the n conductors,

$$[Y_c][V_k] - [I_{km}] = [A]\{[Y_c][V_m] + [I_{mk}]\} \tag{5.51}$$

with $[Y_c] = [Z_c]^{-1}$ = characteristic admittance matrix in phase quantities,

$[A] = e^{-[\gamma]\ell}$ = propagation factor matrix.

Eq. (5.51) is transformed to modal quantities, with

$$[I] = [T_i]\,[I_{mode}] \tag{5.52a}$$

and

$$[V] = [T_i']^{-1}\,[V_{mode}] \tag{5.52b}$$

which yields

$$[I_{km-mode}] = [Y_{c-mode}]\,[V_{k-mode}] - [A_{mode}]\{[Y_{c-mode}]\,[V_{m-mode}] + [I_{mk-mode}]\} \tag{5.53}$$

with both $[Y_{c\text{-mode}}]$ and $[A_{mode}]$ being diagonal matrices,

$$[Y_{c-mode}] = [T_i]^{-1}\,[Y_c]\,[T_i']^{-1} \tag{5.54a}$$

$$[A_{mode}] = [T_i]^{-1}\,[A]\,[T_i] \tag{5.54b}$$

The diagonal element of $[A_{mode}]$ is obtained from the i-th eigenvalue γ_i of the product $[Y'_{phase}]\,[Z'_{phase}]$,

$$A_{mode-i} = e^{-\ell\lambda_i} \tag{5.54c}$$

and $[T_i]$ is the matrix of eigenvectors of the same product $[Y'_{phase}]\,[Z'_{phase}]$. Eq. (5.53) consists of n decoupled (scalar) equations, with one equation for each mode.

Transforming these scalar equations into the time domain is the same procedure as described in Section 4.2.2.6 for the overhead line. For mode i, the second term in Eq. (5.53) is found with the same convolution integral as in Eq. (4.124),

$$hist_{propagation} = -\int_{\tau_{min}}^{\tau_{max}} i_{m-total}(t-u)\,a(u)\,du \quad for\ each\ mode \tag{5.55}$$

with the current $i_{m\text{-total}}$ being the sum of the line current i_{mk} and of a current which would flow through the characteristic impedance of mode i if the voltage v_m of mode i were connected across it. Only known history terms appear in Eq. (5.55), and $hist_{propagation}$ can therefore be found by n recursive convolutions for the n modes, in the same say as in Section 4.2.2.6. The modal propagation factors are very similar in shape to those of an overhead line, as shown for $A_{mode\text{-}3}$ (ω) in Fig. 5.24.

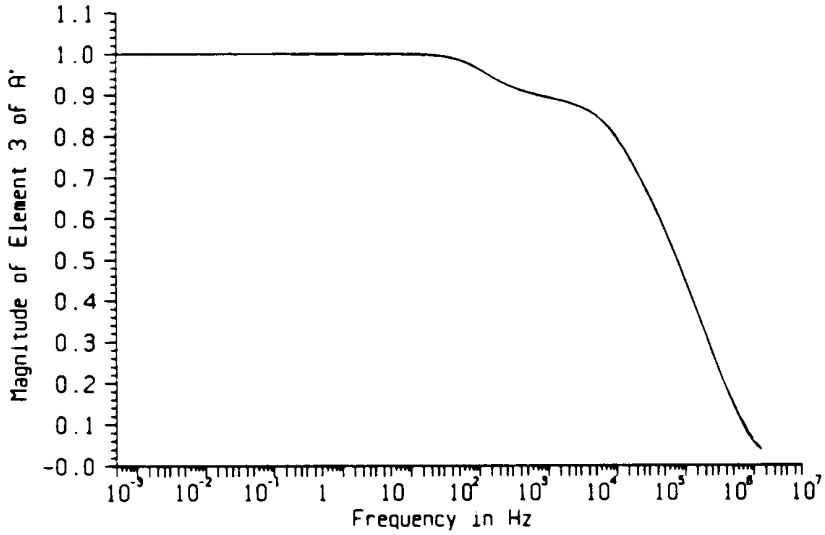

Fig. 5.24 - Magnitude of propagation factor for mode 3 of a 6-conductor system (three single-core cables with core and sheath in each)

With propagation of the conditions from m to k being taken care of through Eq. (5.55), the only unresolved issue in the modal domain equations is the representation of the term Y_cV_k in Eq. (5.53). Again, the frequency dependence of Y_c is similar to that of an overhead line, as shown in Fig. 5.25, and can be represented with the same type of Foster-I R-C network shown in Fig. 4.42(a), and reproduced here as Fig. 5.26. By applying the trapezoidal rule of integration to the capacitances, or by using recursive convolution as discussed in Appendix V, the R-C

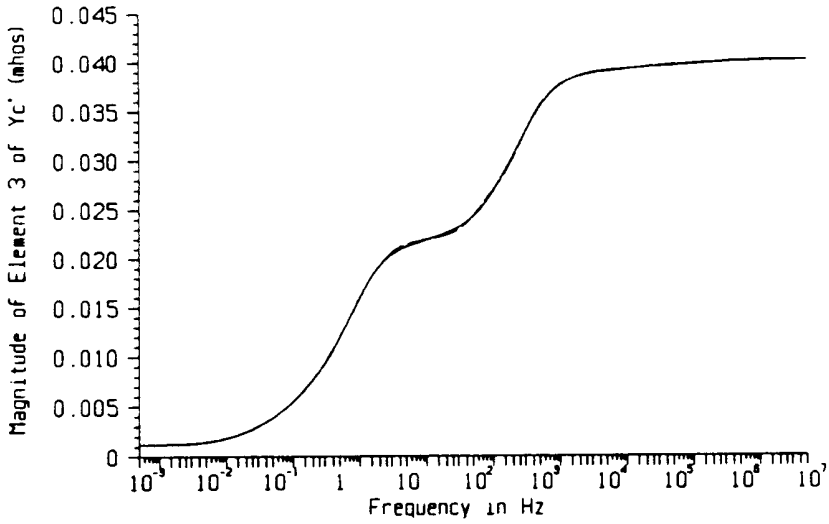

Fig. 5.25 - Magnitude of characteristic admittance for mode 3 (same 6-conductor system as in Fig. 5.24)

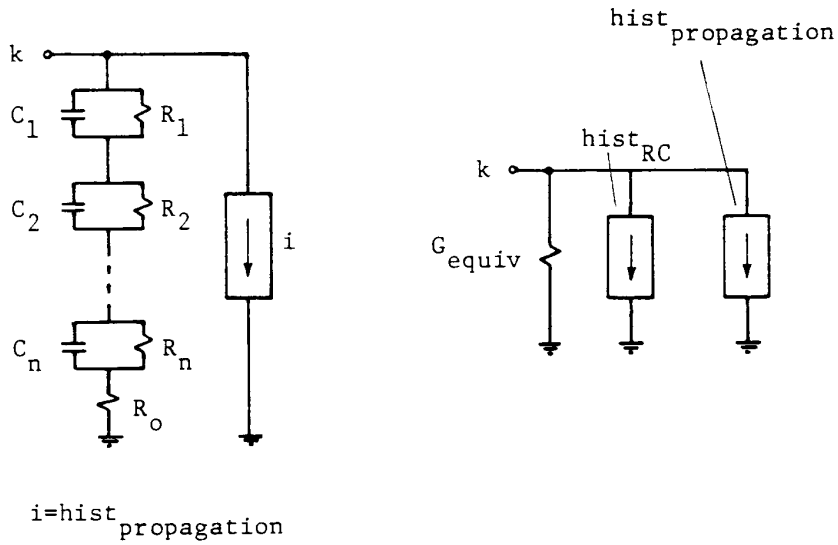

(a) R-C network (b) Equivalent resistance after applying implicit integration to C

Fig. 5.26 - Representation of one mode seen from side k

network is converted into an equivalent conductance G_{equiv} in parallel with a known current source $hist_{RC} + hist_{propagation}$. After the network solution at each time step, the current flowing through the characteristic impedance represented by the R-C network must be calculated for both ends of the cable from $G_{equiv}v + hist_{RC}$, because this term is needed after the elapse of travel time to form the expression $i_{m\text{-}total}$ needed in Eq. (5.55).

From Fig. 5.26(b), it can be seen that each mode is now represented by the scalar, algebraic equation

$$i_{km}(t) = G_{equiv}v_k(t) + (hist_{RC} + hist_{propagation}) \tag{5.56}$$

with an analogous equation for $i_{mk}(t)$ at the other end. If the transformation matrix were constant and real, then Eq. (5.56) could very easily be transformed back to phase quantities,

$$[i_{km\text{-}phase}(t)] = [T_i][G_{equiv}][T_i]^t[v_{k\text{-}phase}] + [T_i][hist]$$

as explained in Eq. (4.109) for the overhead line. As shown in Fig. 5.21, the transformation matrix $[T_i]$ of cables is very much frequency-dependent, and the transformation back to phase quantities now requires convolutions based on Eq. (5.52),

$$[i_{phase}(t)] = \int_{-\infty}^{t} [t_i(t-u)]\,[i_{mode}(u)]\,du \tag{5.57a}$$

$$[v_{mode}(t)] = \int_{-\infty}^{t} [t_i(t-u)]^t\,[v_{phase}(u)]\,du \tag{5.57b}$$

where $[t_i]$ is a matrix obtained from the inverse Fourier transform of the frequency-dependent matrix $[T_i]$. Similar to the curve fitting used for the modal characteristic impedances, each element of $[T_i]$ is again approximated by rational functions of the form

$$T_{\mu\nu}(\omega) = k_0 + \sum_{i=1}^{m} \frac{k_i}{j\omega + p_i} \tag{5.58}$$

with k_0, k_i and p_i being real constants which, when transformed into the time domain, becomes

$$t_{\mu\nu}(t) = k_0\,\sigma(t) + \sum_{i=1}^{m} k_i \exp(-p_i t)\, u(t) \tag{5.59}$$

With the simple sum of exponentials in Eq. (5.59), recursive convolution can be applied again (Appendix V). Then, the convolution integrals in Eq. (5.57) can be split up into a term containing the yet unknown voltages and currents at time t, and the known history terms which can be updated recursively,

$$[i_{phase}(t)] = [t_0]\,[i_{mode}(t)] + [hist_{current}] \tag{5.60a}$$

$$[v_{mode}(t)] = [t_0]^t\,[v_{phase}(t)] + [hist_{voltage}] \tag{5.60b}$$

with $[t_0]$ being a real, constant n x n-matrix. With Eq. (5.60), the transformation of the modal equations (5.56) to phase quantities is now fairly simple,

$$[i_{km-phase}(t)] = [G_{phase}]\,[v_{k-phase}(t)] + [hist_{phase}] \tag{5.61a}$$

with

$$[G_{phase}] = [t_0]\,[G_{phase}]\,[t_0]^t \tag{5.61b}$$

and the history term

$$[hist_{phase}] = [hist_{current}] + [t_0]\{[G_{equiv}][hist_{voltage}] + [hist_{RC}] + [hist_{propagation}]\} \tag{5.61c}$$

Since the form of Eq. (5.61a) is identical to that of Eq. (4.109) for the overhead line with constant $[T_i]$, adding the model to the EMTP is the same as described there. The extra effort lies essentially in the evaluation of the two extra history vectors $[hist_{current}]$ and $[hist_{voltage}]$. After the network solution at each time step, Eq. (5.60) is used to obtain the modal quantities from the phase quantities.

The principle of the frequency-dependent cable model is fairly simple, but its correct implementation depends on many intricacies, which are described in [155]. In particular, it is important to normalize the eigenvectors in such a way that the elements of $[T_i]$ as well as the modal surge admittances $Y_{c\text{-mode-i}}$ both become minimum phase shift functions. This is achieved by making one element of each eigenvector a real and constant number through the entire frequency range. Furthermore, standard eigenvalue/eigenvector subroutines do not produce smooth curves of $[T_i]$ and $[Y_{c\text{-mode}}]$ as a function of frequency, because the order in which the eigenvalues are calculated often changes as one moves from one frequency point to the next. This problem was solved by using an extension of the Jacobi method for complex symmetric matrices. Symmetry is obtained by reformulating the eigenproblem

$$[Y'_{phase}]\,[Z'_{phase}]\,[x] = \lambda[x]$$

in the form

$$[H]\,[r] = \lambda[r] \tag{5.62a}$$

where

$$[H] = [L]^t\,[Z'_{phase}]\,[L] \tag{5.62b}$$

and

$$[x] = [L]\,[r] \tag{5.62c}$$

with [L] being the lower triangular matrix obtained from the Choleski decomposition of $[Y'_{phase}]$ [157]. The Choleski decomposition is a modification of the Gauss elimination method, as explained in Appendix III. One can also replace [L] in Eq. (5.62) with the square root of $[Y'_{phase}]$ obtained from

$$[Y'_{phase}]^{1/2} = [X]\,[\Lambda^{1/2}]\,[X]^{-1} \tag{5.63}$$

where $[\Lambda^{1/2}]$ is the diagonal matrix of the square roots of the eigenvalues, and [X[is the eigenvector matrix of $[Y'_{phase}]$. Both approaches are very efficient if G' is ignored, or if tanδ is constant for all dielectrics in the cable system, because [L] or $[Y'_{phase}]^{1/2}$ must then only be computed once for all frequencies.

For parallel single core cables layed in the ground (not in air), [Y'] is diagonal if loop equations are used. In that case it is more efficient to find the eigenvalues and eigenvectors for $[Y'_{loop}][Z'_{loop}]$, where both [L] and $[Y'_{loop}]^{1/2}$ become the same diagonal matrix with $\sqrt{Y'_{loop\text{-}i}}$ as its elements. The conversion back to phase quantities is trivial with Eq. (5.50).

The reason why the Jacobi procedure produces smooth eigenvectors is that the Jacobi algorithm requires an initial guess for the solution of the eigenvectors. This initial guess is readily available from the solution of the eigenproblem of the preceding frequency step; consequently, the order of the eigenvectors from one calculation to the next is not lost.

Figure 5.27(a) shows the magnitude of the elements of row 3 of the eigenvector matrix $[T_i]$ for the same 6-conductor system as in Fig. 5.24, when standard eigenvalue/eigenvector routines are used. Fig. 5.27(b), on the other hand, shows the same elements of $[T_i]$ calculated with the modified Jacobi algorithm.

As an application for this cable model, consider the case of three 230 kV single-core cables (with core and sheath), buried side by side in horizontal configuration, with a length of 10 km. A unit-step voltage is applied to the core of phase A, and the cores of phases B and C as well as all three sheaths are left ungrounded at both ends. The unit-step function was approximated as a periodic rectangular pulse of 10 ms duration and a period of 20 ms with a Fourier series containing 500 harmonics,

$$v(t) = a_0 + \sum_{i=1}^{500} \{a_i \cos(\omega_i t) + b_i \sin(\omega_i t)\}$$

The wave front of this approximation is shown in Fig. 5.28. Choosing a Fourier series

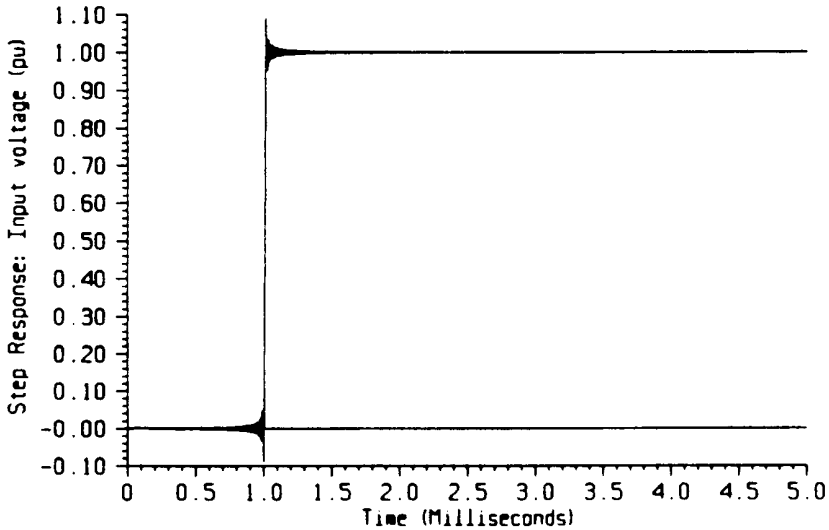

Fig. 5.28 - Fourier series approximation of unit-step

approximation for the voltage source offered the advantage that exact answers could be found as well, by using ac steady-state solutions with exact equivalent π-circuits (Section 4.2.1.3) at each of the 500 frequencies, and by superimposing them. Fig. 5.29 and 5.30 show the EMTP simulation results in the region of the third pulse, superimposed on the exact answers. The two

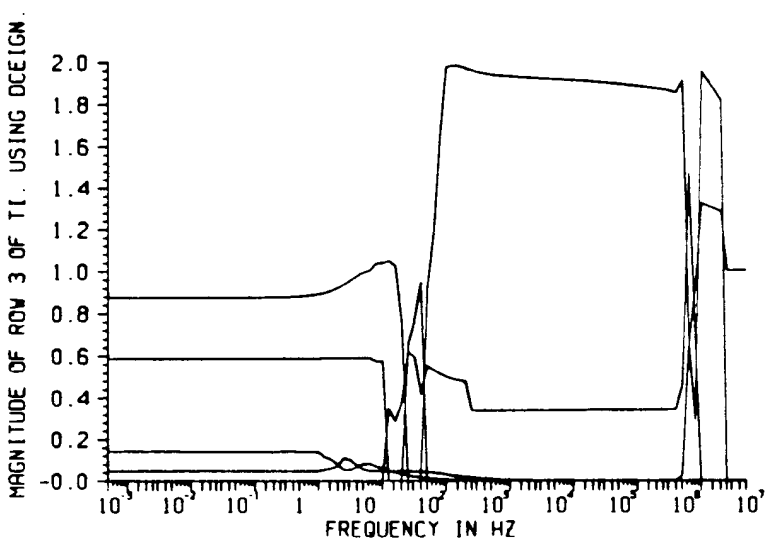

(a) Standard eigenvalue/eigenvector subroutines

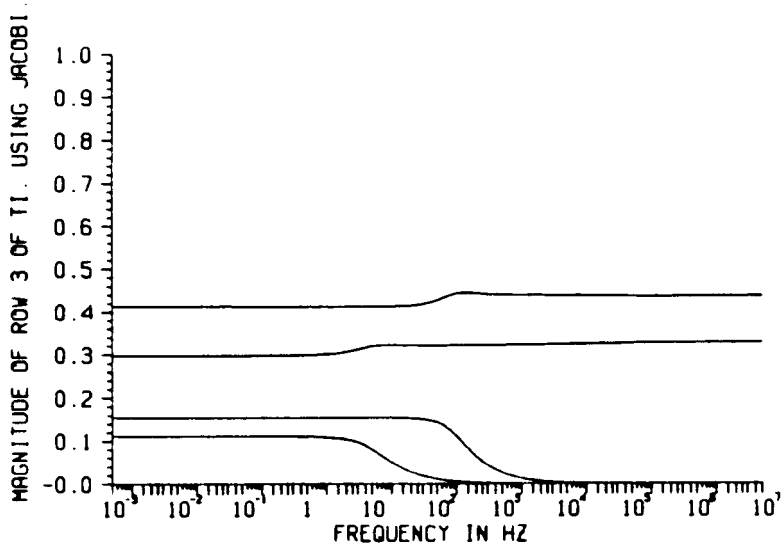

(b) Modified Jacobi algorithm

Fig. 5.27 -
Magnitude of the elements of row 3 of $[T_i]$ (same 6-conductor system as in Fig. 5.24)

curves are indistinguishable in this third pulse region where the phenomena have already become more or less periodic. This shows that the EMTP cable model is capable of producing highly accurate answers. The insert on the right-hand side of Fig. 5.29 shows the response to the first pulse, where the EMTP simulation results differ slightly from the exact answers, not because of inaccuracies in the model but because the EMTP starts from zero initial conditions while the exact answer assumes periodic behavior even for t < 0.

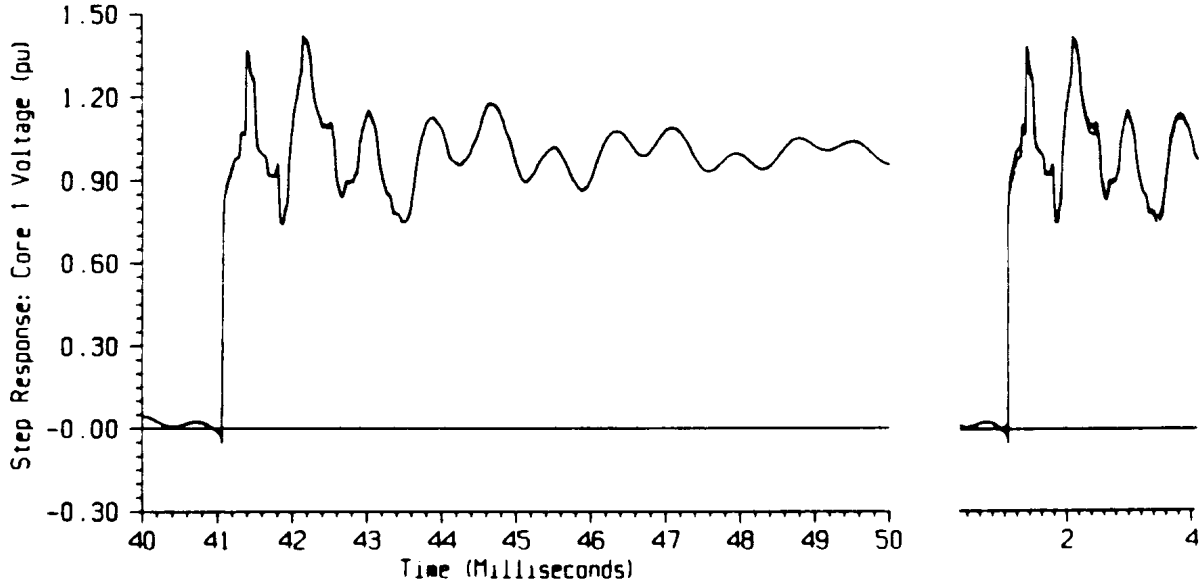

Fig. 5.29 - Step response, receiving end voltage of core (phase A)

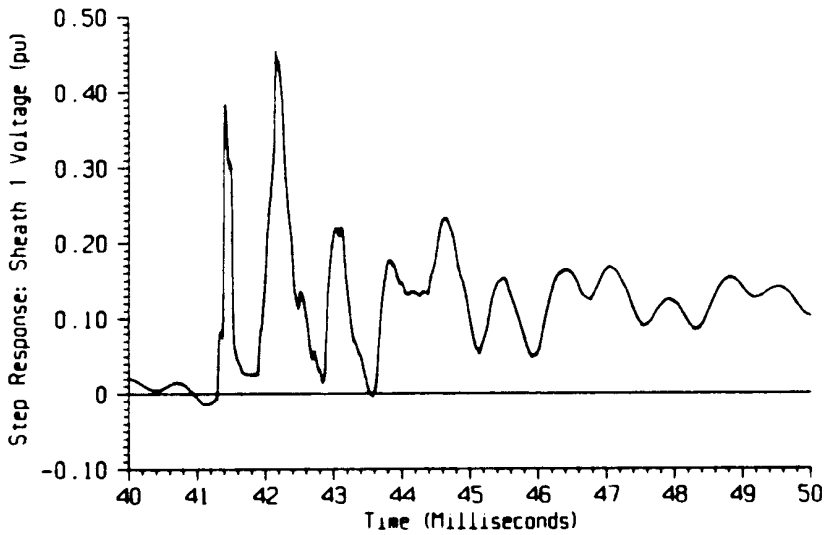

Fig. 5.30 - Step response, receiving end voltage of sheath (phase A)